TRANSMIT ANTENNA SELECTION ALGORITHMS FOR QUADRATURE SPATIAL MODULATION

Suvigya Naidu

Supervisor: Dr. Narushan Pillay

Co-Supervisor: Prof. HongJun Xu

Submitted in fulfilment of the academic requirements of

Master of Science in Engineering

School of Engineering

College of Agriculture, Engineering and Science

University of KwaZulu-Natal

Howard College

South Africa

January 2016

PREFACE

The research contained in this dissertation was completed by the candidate while based in the School of Engineering, Discipline of Electrical, Electronic and Computer Engineering, in the College of Agriculture, Engineering and Science, University of KwaZulu-Natal, Howard College, South Africa. The research was financially supported by Telkom SA SOC Ltd.

The contents of this work have not been submitted in any form to another university and, except where the work of others is acknowledged in the text, the results reported are due to investigations by the candidate.

_____

Signed: Dr. Narushan Pillay

Date:

DECLARATION 1: PLAGIARISM

I, Suvigya Naidu, declare that:

(i) the research reported in this dissertation, except where otherwise indicated or acknowledged, is my original work;

(ii) this dissertation has not been submitted in full or in part for any degree or examination to any other university;

(iii) this dissertation does not contain other persons' data, pictures, graphs or other information, unless specifically acknowledged as being sourced from other persons;

(iv) this dissertation does not contain other persons' writing, unless specifically acknowledged as being sourced from other researchers. Where other written sources have been quoted, then:

a) their words have been re-written but the general information attributed to them has been referenced;

b) where their exact words have been used, their writing has been placed inside quotation marks, and referenced;

(v) where I have used material for which publications followed, I have indicated in detail my role in the work;

(vi) this dissertation is primarily a collection of material, prepared by myself, published as journal articles or presented as a poster and oral presentations at conferences. In some cases, additional material has been included;

(vii) this dissertation does not contain text, graphics or tables copied and pasted from the Internet, unless specifically acknowledged, and the source being detailed in the dissertation and in the References sections.

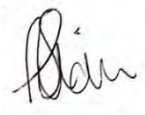

Signed: Suvigya Naidu

Date:

DECLARATION 2: PUBLICATIONS

Chapter 3

1. S. Naidu, N. Pillay, H. Xu, “A Study of Quadrature Spatial Modulation,” in Proceedings of the Southern Africa Telecommunications Network and Applications Conference (SATNAC), pp. 3-8, Aug. 2015.

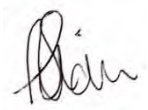

_____

Signed: Suvigya Naidu

Date:

ABSTRACT

The use of multiple-input multiple-output (MIMO) systems has become increasingly popular due to the demand for high data rate transmissions. One such attractive MIMO system is spatial modulation (SM). SM is an ideal candidate for high data rate transmission as it is able to achieve a high spectral efficiency, whilst maintaining a relatively low receiver complexity. SM completely avoids inter-channel interference and the need for inter-antenna synchronisation. Furthermore, SM requires the existence of only one radio frequency chain. However, the need to increase the spectral efficiency achieved by SM is a topic which continues to garner interest.

Quadrature spatial modulation (QSM) was introduced as an innovative SM-based MIMO system. QSM maintains the aforementioned advantages of SM, whilst further increasing the spectral efficiency of SM. However, similar to SM, the need to improve the reliability (error performance) of QSM still exists. One such strategy is the application of a closed-loop technique, such as transmit antenna selection (TAS).

In this dissertation, Euclidean distance-based antenna selection for QSM (EDAS-QSM) is proposed. A substantial improvement in the average error performance is demonstrated. However, this is at the expense of a relatively high computational complexity. To address this, we formulate an algorithm in the form of reduced-complexity Euclidean distance-based antenna selection for QSM (RCEDAS-QSM) that is used for the computation of EDAS-QSM. RCEDAS-QSM yields a significant reduction in the computational complexity, whilst preserving the error performance.

To further address computational complexity, four sub-optimal, low-complexity, TAS schemes for QSM are investigated, viz. capacity optimised antenna selection for QSM (COAS-QSM), TAS for QSM based on amplitude and antenna correlation (TAS-A-C-QSM), low-complexity TAS for QSM based on amplitude and antenna correlation using the splitting technique (LCTAS-A-C-QSM) and TAS based on amplitude, antenna correlation and Euclidean distance for QSM (A-C-ED-QSM).

Amongst the sub-optimal algorithms, A-C-ED-QSM provides superior error performance. While the computational complexity of A-C-ED-QSM is higher than the other sub-optimal, low-complexity schemes, there is a significant reduction in the computational complexity compared to the optimal RCEDAS-QSM. However, this is at the expense of error performance. Hence, clearly a trade-off exists between error performance and computational complexity, and is investigated in detail in this dissertation.

ACKNOWLEDGMENTS

First and foremost, I would like to extend my deepest gratitude to my supervisor, Dr. N. Pillay, for his continuous support and guidance throughout the duration of this research. I would like to thank you for encouraging me to pursue my MSc degree, and for the countless hours you have spent patiently correcting my writing. Your knowledge and commitment to produce work of a high standard has made a life-long impression on me. I would also like to extend a special thanks to my co-supervisor, Prof. H. Xu, for his ever-willingness to share his knowledge and wisdom.

I would like to take this opportunity to extend my appreciation to Telkom SA for financially supporting my research.

To my family, words cannot explain how much your love and support has meant to me. To my parents, without your endless supply of love and words of encouragement, the completion of this dissertation would not have been possible. I would also like to thank my grandmother, who has patiently and unselfishly cared for me throughout my life. To my sisters, Charvinia and Rishaveri, thank you for always providing me with sound advice and hours of laughter.

Lastly, to Rowen, you have inspired and motivated me throughout every stage of my research. Thank you for your unconditional love.

TABLE OF CONTENTS

Page

LIST OF TABLES

Table **Page**

LIST OF FIGURES

Figure **Page**

LIST OF ACRONYMS

A-C-ED-QSM .....Amplitude, Antenna Correlation and Euclidean Distance for QSM
APM .....Amplitude/Phase Modulation
ASM .....Adaptive Spatial Modulation
AWGN .....Additive-White Gaussian Noise
BER .....Bit Error Rate
BiSSK .....Bi-Space Shift Keying
BPSK .....Binary Phase Shift Keying
BLAST .....Bell Labs Layered Space-Time Architecture
COAS .....Capacity Optimized Antenna Selection
COAS-QSM .....COAS for Quadrature Spatial Modulation
DBD .....Distance-Based Ordered Detection
ED .....Euclidean Distance
EDAS .....Euclidean Distance Antenna Selection
EDAS-QSM .....EDAS for Quadrature Spatial Modulation
FBE-SM .....Fractional Bit Encoded Spatial Modulation
flops .....Floating Point Operations
GSM .....Generalised Spatial Modulation
IAS .....Inter-Antenna Synchronisation
ICI .....Interchannel Interference
i.i.d .....Independent and Identically Distributed
ISI .....Intersymbol Interference
LCTAS .....Low-Complexity Transmit Antenna Selection
LCTAS-A-C-QSM .....LCTAS for QSM based on Amplitude and Antenna Correlation
MA-SM .....Multiple Antenna Spatial Modulation
MEA .....Multi-Element Antenna
MIMO .....Multiple-Input Multiple-Output
ML .....Maximum-Likelihood
MOSC .....Modulation Order Selection Criterion
MRC .....Maximum Ratio Combining
OFDM .....Orthogonal Frequency Division Multiplexing
PEP .....Pairwise Error Probability
QAM .....Quadrature Amplitude Modulation
QPSK .....Quadrature Phase Shift Keying
QSM .....Quadrature Spatial Modulation

RCEDAS-QSM .....RCEDAS for Quadrature Spatial Modulation
RF .....Radio Frequency
SD .....Sphere Decoding
SER .....Symbol Error Rate
SM .....Spatial Modulation
SM-OFDM .....SM-Orthogonal Frequency Division Multiplexing
SM-SOMLD .....Soft-Output ML detector for Spatial Modulation
SMUX .....Spatial Multiplexing
SNR .....Signal-to-Noise Ratio
SODBD .....Soft-Output Distance-Based Ordered Detection
SSK .....Space Shift Keying
STBC .....Space-Time Block Coding
STBC-SM .....Space-Time Block Coded Spatial Modulation
SVD .....Signal Vector Based Detection
TAS .....Transmit Antenna Selection
TAS-A-C .....TAS based on Amplitude and Antenna Correlation
TAS-A-C-QSM .....TAS for QSM based on Amplitude and Antenna Correlation
V-BLAST .....Vertical-BLAST

1 INTRODUCTION

Upon reflection on the last three decades, it is glaringly apparent as to why the field of wireless communications has been dubbed as the fastest growing sector of the communications industry. With technology evolving at an exponential pace, the need for the next generation of wireless devices to improve upon their predecessors is of paramount importance. It is vital that each new wireless device shows significant improvement in terms of link communication speed, link reliability and enhanced spectral efficiency [1]. However, communication through a wireless medium remains a challenging task due to the impairment suffered by the wireless signal. The deterioration of this signal can be attributed to the effects imposed by noise, attenuation, distortion and interference [1]. Hence, it is clear that the dominant consideration in wireless technology is to employ a system that is able to mitigate these impairments.

The advent of multiple-input multiple-output (MIMO) technology came about through the necessity to mitigate the negative effects of the wireless channel, whilst striving to increase data throughput [1]. The concept of utilising a multi-element antenna (MEA) system in a Rayleigh fading environment was first proposed in 1987 [2]. Raleigh *et. al.* and Foschini then further expanded upon this concept in [3] and [4], respectively. This MEA system became known as MIMO technology and was described by Foschini [4] as an architecture, which employed an antenna array at both the transmitter and receiver.

Figure 1.1 depicts a MIMO system with N_T transmit and N_R receive antennas. By employing MIMO architecture, the transmitted data can traverse through several channels in order to arrive at the receiver. Assuming that all channels are independent, or have a low correlation, there is a minimal chance that all the channel links will fail [1].

The received signal vector for an $N_T \times N_R$ MIMO system is [5]:

$$\boldsymbol{y} = \boldsymbol{H}\boldsymbol{x} + \boldsymbol{n} \tag{1.1}$$

where $\boldsymbol{x}$ is an $N_T \times 1$ transmit symbol vector and $\boldsymbol{n}$ is an $N_R \times 1$ additive white Gaussian noise (AWGN) vector. $\boldsymbol{H} = [\boldsymbol{h}_1 \ \boldsymbol{h}_2 \ \cdots \ \boldsymbol{h}_{N_T}]$ represents an $N_R \times N_T$ channel gain matrix and $\boldsymbol{h}_j$ is an $N_R \times 1$ column of $\boldsymbol{H}$, where $j \in [1: N_T]$. h_{kj} signifies the gain from transmit antenna j to receive antenna k, where $j \in [1: N_T]$ and $k \in [1: N_R]$.

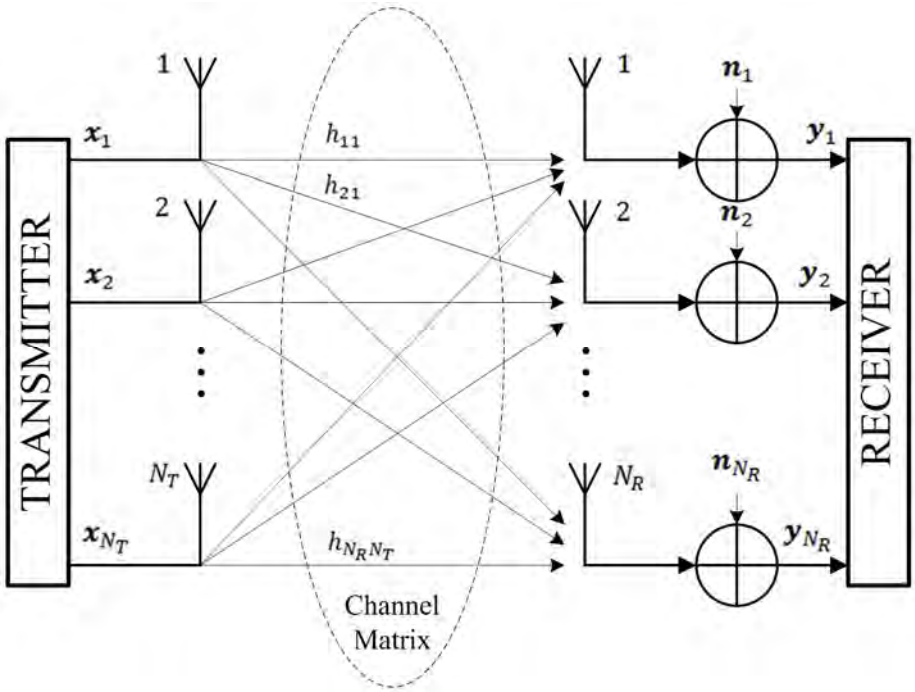

Figure 1.1 Illustration of an $N_T \times N_R$ MIMO system [1, 5]

The allure of employing MIMO architecture lies in the fact that one can either improve error performance through increasing the diversity gain, or alternatively, increase the overall throughput by making use of multiplexing [5]. A MIMO system in the presence of an uncorrelated Rayleigh-fading environment has the potential to provide an extremely large gain in channel capacity, as well as a significant increase in the spectral efficiency of the system [6]. Channel capacity is defined as the maximum data rate that is transmitted over a channel whilst maintaining a minimal error probability [5]. Spectral efficiency, however, refers to the number of information bits that can be transmitted over a single channel use [1]. In addition, intersymbol interference (ISI), along with interference from other users, can be reduced by using MIMO systems [5].

Although employing multiple transmit and receive antennas can provide large spectral efficiencies and channel gains, there are a few areas of concern when dealing with MIMO systems. Comparing a highly correlated multipath fading environment, to one that is independent and identically distributed (i.i.d), there is a noticeable loss in the expected capacity gain of the system [7]. High correlation between antenna elements can be caused by insufficient spacing between said antenna elements [7]. Additionally, the capacity gain achieved by a MIMO system also depends on the algorithm used for detection at the receiver side. MIMO systems suffer from high interchannel interference (ICI) at the input of the receiver. In order to reduce ICI, and consequently prevent the loss of channel capacity, an adequate detection algorithm should be implemented at the receiver [4].

Bell Labs layered space-time architecture (BLAST) was introduced as an attractive MIMO architecture [4]. This promising wireless communication architecture gave rise to a simplified version of BLAST, known as vertical-BLAST (V-BLAST). By using the BLAST approach, coupled with the V-BLAST detection scheme, MIMO systems operating in an ideal environment were capable of achieving spectral efficiencies that had previously been unprecedented [8]. However, there exists several challenges surrounding BLAST. The detection algorithm used by BLAST to reduce ICI is highly complex, and thus, increases the computational complexity of the system [9]. Moreover, although V-BLAST performed well in ideal conditions, it was shown in [10] and [11] that the performance of V-BLAST deteriorates in non-ideal circumstances.

In order to alleviate the difficulties associated with MIMO technology and in particular, BLAST techniques, an innovative wireless communication scheme known as spatial modulation (SM) was proposed by Mesleh *et. al.* [12].

1.1 Spatial Modulation

SM was proposed by Mesleh *et. al.* [12] as a pioneering MIMO system that capitalises on the increased spectral efficiency achieved by V-BLAST, whilst simultaneously improving the achievable error performance of prior MIMO systems.

For conventional MIMO systems, each symbol is part of a symbol set and is modulated using various techniques, such as quadrature amplitude modulation (QAM) or quadrature phase shift keying (QPSK). Each symbol then represents a constellation point in the two dimensional signal plane. However, the principle behind SM is to take into consideration the inclusion of a third dimension, known as the spatial dimension [9, 12-14].

For SM, at any given interval, only one transmit antenna is active. SM utilises the active transmit antenna index as an additional source of information, which is added to the transmitted bit stream. During each transmission, the dormant antennas transmit zero power. By doing this, ICI at the receiver is completely avoided, which results in a relatively low receiver complexity [9, 12]. Furthermore, due to only one transmit antenna being active per time slot, correlation or inter-antenna synchronisation (IAS) between transmit antennas is not required [9, 12]. Having only one active transmit antenna also ensures that only one radio frequency (RF) chain is required at the transmitter. Not only does SM achieve a relatively high spectral efficiency, it also improves the error performance achieved by V-BLAST [9, 12-14].

SM has proven to be an attractive wireless communication scheme that has been widely recognised for its many merits. However, there are issues which plague SM that must be rectified in order to realise its full potential, viz.:

i. The spectral efficiency of SM is limited and is only able to increase in proportion to the base-two logarithm of the number of transmit antennas [9, 12].
ii. In order for SM to achieve optimal error performance, the maximum-likelihood (ML) algorithm must be employed at the receiver. Unlike alternate MIMO systems, whose complexity increases exponentially with N_T, the complexity of ML-based SM detection increases linearly with respect to N_T. Therefore, compared to the ML detection of other MIMO systems, the ML-based SM detector is relatively low in complexity. In spite of this, the complexity of optimal SM detection remains considerably high [9, 12-14].
iii. Lastly, due to SM employing only one active transmit antenna, it is not able to exploit the transmit diversity gains achieved in other MIMO systems [9, 12].

Several adjustments and additions have been made to SM in a bid to rectify the abovementioned issues. A selection of these schemes have been chronicled in the sub-sections that follow. These schemes either address the receiver/hardware complexity of SM, the spectral efficiency of SM or the transmit diversity of SM. First, a survey of various schemes which reduce either the hardware or receiver complexity of SM is presented. This is followed by a review of several SM-based schemes, which focus on the need to improve the spectral efficiency and increase the transmit diversity of SM. Based on their design, these schemes are then classified as either open-loop SM or closed-loop SM. Open-loop design refers to a system in which the information at the receiver has no effect at the transmitter. Conversely, closed-loop design makes use of a feedback system which utilises channel state information at the transmitter.

1.1.1 Complexity Reducing Techniques for SM

In [9, 12], Mesleh *et. al.* proposed an SM detection scheme which was based on the use of maximum ratio combining (MRC) at the receiver. MRC-based SM detection initially estimates the transmit antenna index, which is then used in order to detect the information symbol [9, 12]. Upon further investigation, Jeganathan *et. al.* [13] proved the MRC-based method of detection to be sub-optimal. Therefore, [13] presented the concept of the ML algorithm as an optimal SM detector. The ML-based SM detector achieves optimal error performance by performing an exhaustive search to jointly estimate the transmit antenna index and symbol [13]. As a consequence, the computational complexity of the ML algorithm is exceptionally high.

In order to address the high computational complexity associated with the ML-based SM detector, several alternate detectors for SM have been proposed. A selection of these SM detectors, along with schemes that reduce the hardware complexity of SM, have been chronicled in the sub-sections that follow.

1.1.1.1 Distance-Based Ordered Detection

In a bid to reduce the complexity of ML-based SM detection, whilst maintaining near-ML performance, the authors of [15] have proposed a distance-based ordered detection (DBD) algorithm for SM. For DBD, the symbol from each transmit antenna index in the antenna array is first computed and then used to determine the corresponding transmit symbol estimate. These transmit symbol estimates are then compared with the received signal vector. The closest estimate is used to jointly determine the final estimates of the active transmit antenna index and transmit symbol [15]. Unlike the ML-based detector, which searches through MN_T points, DBD only searches through a maximum of N_T points [15]. Therefore, it is evident that the complexity of DBD is significantly reduced compared to ML detection.

Due to ML-based detection operating on a hard decision basis, a soft-output ML detector for SM (SM-SOMLD) was proposed by Hwang *et. al.* [16]. Under coded channel conditions, the SM-SOMLD [16] was shown to outperform the traditional ML-based detector in [13]. Although the error performance of SM-SOMLD was favourable, it continued to suffer from high computational complexity. In order to remedy this, the authors of [15] further presented a low-complexity, soft-output DBD (SODBD) algorithm. The use of SODBD for SM under coded channel conditions, is favourable as it achieves near-ML performance at a substantial reduction in computational complexity [15].

1.1.1.2 Sphere Decoding Detection

Sphere decoding (SD) was initially proposed as an innovative SM detection algorithm by Younis *et. al.* [17]. Unlike conventional ML-based SM detection, the SD algorithm avoids an exhaustive search by only examining the points which lie within a sphere of a specified radius, centred at the received signal [17]. Thereby, the proposed SD algorithm reduces the receiver complexity of optimal SM detection [17].

The SD-based algorithm for SM reduces the complexity of ML-based detection by no less than 45%, whilst maintaining near-optimal error performance [17]. However, it is also noted that for a small number of receive antennas, the computational complexity of the SD algorithm considerably increases [16].

1.1.1.3 Signal Vector Based Detection

Signal vector based detection (SVD) was introduced as an efficient, low-complexity algorithm, which maintained the high transmission rate of SM [18, 19]. The core concept of SVD is that the estimated transmit antenna index corresponds to the channel vector that forms the smallest included angle with the received signal vector [18, 19]. In other words, SVD determines the active transmit antenna index by selecting the channel gain vector which forms the smallest included angle with the received signal vector. Once an estimate of the antenna index is achieved, a traditional QAM demodulator is used to achieve an estimate of the transmit symbol [18].

Although the complexity of SVD is significantly lower than ML detection, the performance loss of SVD is exceptionally large [19]. To counteract this deterioration in error performance, signal vector based list detection, or list SVD, was introduced as an effective variation of SVD [20]. List SVD requires a two-step detection process: first, a list of the $'L'$ candidate antennas, which form the $'L'$ smallest angles with the received signal, is created. Next, based on the list of candidate antenna indices, transmit symbol detection is performed [20]. For a small list size, the error performance of list SVD is close to that of optimal ML detection. However, when compared to conventional SVD, the improved error performance of list SVD is accompanied by an increase in complexity [20].

1.1.1.4 Space Shift Keying Modulation/Bi-Space Shift Keying Modulation

Although space shift keying (SSK) modulation does not fall under the scope of SM detection, the implementation of SSK was found to be very low in complexity. As a result, SSK reduced the hardware complexity, and cost, of SM [21].

Unlike conventional amplitude/phase modulation (APM) techniques, such as SM, SSK modulation utilises the spatial domain as the only means of relaying information [21]. Although based on the concept of SM, SSK does not use transmitted symbols in order to convey information. Instead, SSK employs the use of antenna indices to transmit information [21].

Eliminating the use of APM has shown to be favourable, especially in terms of reducing complexity at the detector. Due to the simple nature of SSK modulation, the complexity at the detector is significantly reduced [21]. When using SSK modulation, the phase and amplitude of the signal does not convey any information. As a result, the criteria for the transceiver is less stringent, and a variety of options can be explored, including the use of non-coherent detectors [21]. Since only one transmit antenna is active during each transmission period, the elimination of ICI at the receiver, and other aforementioned advantages of SM, are maintained.

Although SSK has shown to be advantageous in certain aspects, it must be noted that the issues associated with SM has not been fully addressed by this scheme. The error performance of SM did not improve when SSK modulation was used [21]. Additionally, the number of transmit antennas for SSK can be impractically large for high data rates, rendering it unsuitable for use in small mobile stations [21]. Lastly, the potential for transmit diversity gain has still not been exploited by SSK.

In order to address the shortcomings of SSK, bi-space shift keying (BiSSK) was proposed as a new, SSK-based scheme in [22]. BiSSK was proposed as a novel scheme which maintained the benefits of SSK, such as low detection complexity, whilst doubling the spectral efficiency of SSK [22]. The principle behind BiSSK was to simultaneously employ the use of two transmit antennas. The first antenna would transmit the real part of a transmit symbol, whilst the second antenna would transmit the imaginary part of the symbol [22]. By employing this technique, BiSSK was able to transmit twice the amount of data as SSK. Hence, the spectral efficiency of BiSSK is twice that of SSK.

As previously mentioned, the limited spectral efficiency of SSK made it impractical for high data rate usage. However, the increase in spectral efficiency offered by BiSSK rectified this limitation. A prominent drawback of BiSSK was that it only improved upon SSK in terms of increasing the spectral efficiency of SSK. BiSSK did little for the error performance of SSK. For identical hardware configurations, the use of BiSSK results in a slight loss in overall system performance [22].

1.1.2 Open-loop Design for SM

The following schemes are based on SM and fall under the categorisation of open-loop design. Open-loop SM refers to a MIMO system, where the transmitter does not receive any feedback.

1.1.2.1 SM-Orthogonal Frequency Division Multiplexing

SM-Orthogonal Frequency Division Multiplexing (SM-OFDM) is a promising, spectrally efficient, multiple-antenna technique which combines SM with orthogonal frequency division multiplexing (OFDM) [23, 24]. SM-OFDM increases the spectral efficiency of SM, whilst simultaneously mitigating the effects of a frequency-selective fading channel by dividing the channel into parallel frequency flat-fading sub-channels [23, 24]. In doing so, the available bandwidth is efficiently utilized and reliable high speed transmission is made possible.

For SM-OFDM, each sub-channel is mapped to a transmit antenna number. Furthermore, at any instant of time, only one transmit antenna is capable of transmitting data on a particular sub-channel [23, 24]. Therefore, SM-OFDM is able to completely avoid ICI at the receiver and the need for IAS at the transmitter. Lastly, the authors of [16] demonstrated that the BER performance of SM-OFDM operated using soft-output ML detection is superior to that of conventional SM with ML detection. Therefore, it can be concluded that SM-OFDM is a viable, spectrally efficient, MIMO scheme that is capable of improving the BER performance of SM.

1.1.2.2 Fractional Bit Encoded Spatial Modulation

It is often impractical to implement SM in scenarios where compact mobile devices impose space constraints. This is due to the restriction that for SM, the number of transmit antennas present must be a power of two. Fractional bit encoded spatial modulation (FBE-SM) was proposed by Serafimovski *et. al.* [25] in order to overcome this limitation.

FBE-SM relies on the application of modulus conversion in order to achieve a fractional bit rate. By doing this, FBE-SM allows a fraction of bits, or a non-integer number of bits, to be mapped to a constellation point in the spatial domain. This allows for the antenna index to be encoded with a non-integer number of bits, whilst the encoding process in the signal domain remains unchanged [25].

FBE-SM was introduced as a flexible MIMO scheme, which enabled the use of an arbitrary number of antennas at the transmitter. FBE-SM makes use of the theory of modulus conversion in order to achieve a system that is better suited for compact wireless devices. However, a notable drawback of this approach is that it is predisposed to performance degradation due to the effects of error propagation [25]. In addition, similar to SM, FBE-SM does not exploit the potential for transmit diversity gain.

1.1.2.3 Generalised Spatial Modulation

As previously discussed, SM is limited in the sense that its spectral efficiency is proportionate to the base-two logarithm of the number of transmit antennas. Generalised spatial modulation (GSM) was proposed in order to alleviate this limitation, as well as to diminish the error propagation suffered by FBE-SM [26, 27].

GSM activates multiple transmit antennas with the intention of simultaneously transmitting the same data symbol from these antennas [26, 27]. By employing this technique, GSM is able to reduce the number of transmit antennas required to achieve the same spectral efficiency as SM. Furthermore, GSM is also able to avoid ICI at the receiver. By concurrently transmitting the same

data symbol from multiple transmit antennas, GSM increases both the transmit diversity gain, as well as the reliability of the wireless channel [26].

GSM achieves a higher spectral efficiency than SM by mapping information bits to the index of a combination of transmit antennas. Although GSM increases the spectral efficiency of SM, room for improvement still exists. In order to avoid ISI, IAS between the active transmit antennas is required. Additionally, the complexity of GSM increases as the number of transmit antennas increases. Lastly, when compared to SM, the BER performance of GSM was equivalent, at best [26].

1.1.2.4 Multiple Active Spatial Modulation

Multiple active spatial modulation (MA-SM) was proposed in [28] as a novel multi-antenna scheme which served as an extension of GSM. As previously mentioned, GSM simultaneously activates several transmit antennas during each time interval. Using the principle of SM, each active antenna then transmit the same information symbol [26]. Similarly to GSM, MA-SM allows the simultaneous activation of multiple transmit antennas. However, the key difference between MA-SM and GSM is that for MA-SM, each transmit antenna carries a different information symbol [28].

In contrast to the ML detection algorithm used by GSM, MA-SM employs the use of a near-optimal, low-complexity detector [28]. In doing so, the computational complexity imposed by the receiver is significantly reduced. Furthermore, in uncorrelated channels, MA-SM is shown to have improved the error performance of SM and GSM [28]. However, it must be noted that although MA-SM has increased the spectral efficiency of SM, its error performance is prone to severe deterioration, especially when a large number of active transmit antennas are employed [28].

1.1.2.5 Space-Time Block Coded Spatial Modulation

Space-time block coded spatial modulation (STBC-SM) was introduced by Basar *et. al.* in [29]. STBC-SM makes use of APM techniques, as well as the spatial domain, in order to relay information. Alamouti's code is employed as the space-time block coding (STBC) matrix, which conveys information and exploits the transmit diversity potential of MIMO channels [29]. In the STBC-SM scheme, Alamouti's STBC matrix embeds two complex data symbols and the indices of the two active transmit antennas for transmission on the wireless channel.

STBC-SM has significant performance advantages over conventional SM. Not only does STBC-SM have a higher spectral efficiency than SM, but it also capitalises on the diversity

advantage of STBC [29]. The linear increase in decoding complexity of STBC-SM is negligible when the scheme's significant improvement in bit error rate (BER) performance is taken into consideration. Furthermore, due to the orthogonality of Alamouti's STBC, ICI at the receiver is eliminated, and IAS between transmit antennas is not required.

STBC-SM has proven to be a suitable scheme for high-rate, low-complexity wireless communications. However, two RF chains, which can be both bulky and expensive, are required for transmission when using STBC-SM [29].

1.1.2.6 Quadrature Spatial Modulation

Due to the demand for high data rate wireless communication, boosting the spectral efficiency of SM has gained significant interest in recent literature. Quadrature spatial modulation (QSM) was proposed by Mesleh *et. al.* [30, 31] as a new, spectral efficiency enhancing, technique based on SM.

The essential difference between QSM and SM lies in the processing of the spatial constellation symbol prior to transmission. SM transmits the constellation symbol from one antenna, thereby avoiding ICI at the receiver. Conversely, QSM expands the data symbol into its real and imaginary components before simultaneously transmitting these components from one or two antennas. The real and imaginary, or in-phase and quadrature-phase, components of a data symbol are orthogonal. Therefore, QSM maintains the avoidance of ICI at the receiver [30, 31].

In order to transmit simultaneously, QSM requires the transmit antennas to be synchronised. However, this compromise is insignificant in comparison to the benefits offered by QSM. By expanding the data symbol prior to transmission, QSM increases the spectral efficiency of SM by $\log_2 N_T$ bits. Additionally, QSM improves the error performance of SM. These advantages are achieved at no extra expense, i.e. QSM and SM have been proven to have equivalent receiver complexity [30, 31].

1.1.3 Closed-loop Design for SM

The following SM-based schemes employ a closed-loop design, which as mentioned previously, relies on channel state information sent to the transmitter.

1.1.3.1 Adaptive Spatial Modulation

Adaptive spatial modulation (ASM) was proposed in [32] as a novel MIMO scheme which would improve the BER performance of conventional SM. ASM explored the idea that using transmit and receive optimisation techniques could improve the performance of a wireless system. Based

on this concept, ASM proposed the use of a modulation order selection criterion (MOSC), which minimises the conditioned pairwise error probability (PEP) for each channel realisation [32].

In contrast to SM, which uses the same modulation order for data mapping, ASM suggests that based on channel conditions, a MOSC assigns the modulation order to the transmit antennas. This low-complexity MOSC determines the optimal modulation order for each transmit antenna that yields the best system performance [32].

ASM significantly improves the BER performance of SM, especially at high signal-to-noise ratio (SNR) values. Conversely, ASM does not benefit from the spatial freedom offered by SM. This is because, unlike ASM, SM has the potential to improve error performance by varying the number of transmit antennas and the size of the signal constellation [33]. Moreover, not only does ASM suffer from high system complexity, it does not exploit the ability of MIMO systems to achieve transmit diversity gains.

1.1.3.2 Transmit Antenna Selection for Spatial Modulation

In recent years, the use of transmit antenna selection (TAS) for MIMO systems has shown to be extremely beneficial. Selecting a subset of antennas can be especially useful for link initialisation, link maintenance, or for the partial handoff of substreams [34, 35]. Furthermore, employing TAS has proven to reduce hardware complexity and cost, achieve full diversity and increase gain capacity [36].

TAS was first used in [37] as a technique to increase the capacity of MIMO systems. In [37] it was shown that when the channel matrix is ill-conditioned, using fewer transmit antennas can increase the capacity of the system. TAS was founded on two assumptions, viz. the channel at the receiver is known, and there exists a limited feedback path from the receiver to the transmitter. Based on the selection criterion, the feedback path from the receiver to the transmitter conveys the set of transmit antennas which yield optimal system capacity. Optimal capacity is achieved when the selection of transmit antennas yields the largest capacity than any other configuration using the same number of transmit antennas [37].

The selection criterion proposed in [37] was based on the Shannon capacity, and as such, yielded optimal capacity gain. However, [34, 35] presented a selection criterion which minimised the probability of symbol error rate (SER) for spatial multiplexing (SMUX) systems. TAS which maximised the minimum Euclidean distance (ED) of a received constellation, yielded optimal error performance. ED is a function of both the received constellation and channel. As a result, the ED criterion selects an optimal antenna subset in terms of the minimum error rate [34, 35].

In [34, 35], it was shown that making use of TAS can improve the performance of MIMO systems. Based on this, [38] showed that employing a similar TAS technique can significantly enhance the error performance of SSK. Furthermore, [34, 35] showed that the availability of additional antennas can be used as an inexpensive way of exploiting diversity advantage. This was corroborated in [38], whilst further proving that the diversity of SSK can be improved by increasing the number of surplus transmit antennas.

Proposing a link-adaptation scheme, or TAS, to obtain superior system performance for SM transmission was conceived in [33]. Maximising the minimum ED among the legitimate transmit vectors was used as the decision metric for optimal antenna selection in [33] and [39]. This proposed TAS scheme offered a significant SNR gain with respect to conventional SM. Not only did combining TAS with SM improve error performance, it increased the diversity order of SM as well as its robustness against spatial correlation [33, 39].

1.2 Motivation and Research Objectives

As previously stated, SM has three inherent limitations, viz. the increased receiver complexity associated with ML detection, its limited spectral efficiency and the fact that SM has no transmit diversity. QSM has been proposed as a novel scheme, which, by relatively simple means, increases the spectral efficiency of SM, as well as, improves the BER performance achieved by SM. More recently, closed-loop techniques, such as transmit antenna selection, were utilised to increase the transmit diversity of conventional SM systems [39, 40]. In these techniques, the SM transmitter relied on feedback from the receiver. In existing literature, the transmit diversity gain of the QSM scheme operating in a closed-loop scenario was not considered [30, 31].

Utilising the minimum ED among all transmit vectors was first implemented as a criterion for TAS in [33]. Here it was noted that applying Euclidean distance based antenna selection (EDAS) to SM resulted in a significant improvement in error performance [33]. However, implementing EDAS requires an exhaustive search, which is extremely high in computational complexity, and often makes EDAS unrealistic to implement. With this in mind, [39, 41] have proposed an approach which reduces the overall computational complexity of EDAS, whilst maintaining optimal error performance. Although EDAS is an optimal antenna selection technique, applying it to QSM would render an impractically high computational complexity. Thus, reducing the complexity of EDAS when applied to QSM is imperative.

Although EDAS is an optimal approach for antenna selection, it has been shown to be unsuitable for low-complexity applications. The authors of [39, 41] demonstrated that the error performance of SM can still be improved by employing sub-optimal, low-complexity, antenna selection. However, it is noted that this improvement is not as substantial as that achieved by the optimal approach for TAS. In addition to this, [39, 42] have showed that employing low-complexity transmit antenna selection (LCTAS) can improve error performance, while limiting computational complexity. On this note, applying LCTAS to QSM must be further explored.

1.3 Research Contributions

i. The first contribution of this dissertation is to improve the error performance of QSM by implementing a closed-loop approach. This is achieved through the use of transmit antenna selection, and consequently, transmit diversity gains are achieved. This dissertation first proposes that the EDAS technique be applied to QSM so as to yield optimal error performance. Due to the high computational complexity imposed by optimal TAS, reduced-complexity EDAS for QSM (RCEDAS-QSM) is presented as a low-complexity, optimal TAS scheme. Lastly, this dissertation further proposes the application of four sub-optimal, LCTAS techniques to the QSM scheme. The first antenna selection technique is capacity optimized antenna selection for QSM (COAS-QSM) [39, 43], the second is TAS for QSM based on amplitude and antenna correlation (TAS-A-C-QSM) [42-44], the third antenna selection scheme is low-complexity TAS for QSM based on amplitude and antenna correlation using the splitting technique (LCTAS-A-C-QSM) [42, 43], whilst the final scheme is TAS for QSM based on amplitude, antenna correlation and Euclidean distance (A-C-ED-QSM) [42]. The error performance of each of the above-mentioned TAS algorithms are then compared.

ii. The second contribution of this dissertation is to formulate the computational complexity imposed by the optimal TAS algorithms, i.e. EDAS-QSM and RCEDAS-QSM. Furthermore, the computational complexity of the four sub-optimal, LCTAS schemes is evaluated and compared to that of EDAS-QSM and RCEDAS-QSM. The computational complexity of each TAS algorithm is computed in terms of the number of floating point operations (flops).

1.4 Contribution to the Literature

i. S. Naidu, N. Pillay, H. Xu, "A Study of Quadrature Spatial Modulation," in Proceedings of the Southern Africa Telecommunications Network and Applications Conference (SATNAC), pp. 3-8, Aug. 2015 (Received an award for the best paper presented at SATNAC).

ii. S. Naidu, N. Pillay, H. Xu, "Transmit Antenna Selection Schemes for Quadrature Spatial Modulation," (in preparation, to be submitted to IET Communications).

1.5 Outline of Dissertation Structure

The remainder of this dissertation is structured as follows: Chapter 2 and Chapter 3 focuses on the system model, as well as provides further background, on SM and QSM, respectively. Furthermore, these chapters also present an analysis of the simulated and analytical results for SM and QSM. Chapter 4 discusses both optimal and sub-optimal TAS for QSM, including the computational complexity imposed by these schemes. Additionally, Monte Carlo simulations of each TAS algorithm is presented and compared with conventional QSM. Finally, Chapter 5 draws conclusions, documents the contributions of this research, as well as proposes future work that can be conducted in this field.

1.6 Notation

Bold italics upper/lower case symbols denote matrices/vectors, while regular letters represent scalar quantities. We use $[\cdot]^T$, $(\cdot)^H$, $E[\cdot]$, $|\cdot|$ and $\|\cdot\|_F$ for transpose, Hermitian, expectation, Euclidean norm and Frobenius norm operators, respectively. $R\{\cdot\}$ represents the real part of a complex argument, i represents a complex number and $(\cdot)^*$ represents the complex conjugate of a number. $\min_{w}(\cdot)$ and $\operatorname{argmin}_{w}(\cdot)$ both represents the minimum of an argument with respect to w. Lastly, $\operatorname{argmax}_{w}(\cdot)$, $\binom{\cdot}{\cdot}$, $\min(\cdot)$ represents the maximum of an argument with respect to w, the binomial coefficient and the minimum value of an argument, respectively.

2 SPATIAL MODULATION

This section serves to provide as an overview of the SM scheme. Further explanations of the SM system model, detection scheme and analytical performance can be found in the succeeding subsections.

2.1 System Model

The SM system model, shown in Figure 2.1, consists of a MIMO wireless link with N_T transmit and N_R receive antennas [12].

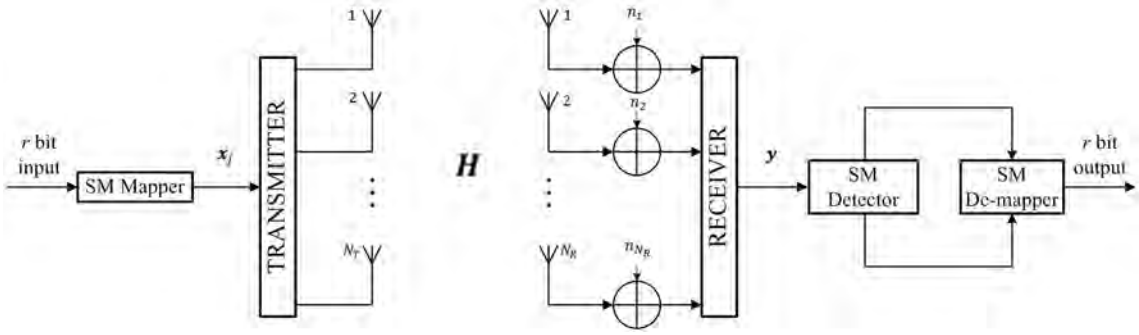

Figure 2.1 SM system model [12]

An $r = \log_2(MN_T)$ bit binary input is fed to the SM mapper, where the transmit antenna index j, $j \in [1: N_T]$, transmits an M-*ary* QAM symbol x_q, $q \in [1: M]$.

The output of the SM mapper is given by [9, 12]:

$$\boldsymbol{x}_j = \begin{bmatrix} 0 & 0 & \cdots & x_q & \cdots & 0 & 0 \end{bmatrix}^T \tag{2.1}$$

(1^{st} position, $N_T{}^{th}$ position, j^{th} position)

where $\boldsymbol{x}_j$ is the $N_T \times 1$ transmit vector and x_q denotes a symbol from the Gray-coded, M-QAM constellation, with $E\left[\left|x_q\right|^2\right] = 1$. Due to the nature of SM, only one transmit antenna remains active during each transmission. As a result, only one element in the signal vector $\boldsymbol{x}_j$ is non-zero. This non-zero entry is located at the j^{th} position of $\boldsymbol{x}_j$ and corresponds to the active transmit antenna [9, 12].

Based on the Gray-coded constellation points in Table 2.1, an example of the SM mapping process is shown in Table 2.2, for 4-QAM SM, where $N_T = 4$. The first $\log_2 N_T$ bits represents the antenna index j, whilst the remaining $\log_2 M$ bits denotes the M-QAM symbol to be transmitted.

Table 2.1 Gray-coded constellation points for 4-QAM

$\log_2 M$ bits	M-QAM Symbol
0 0	$x_q = +1 + 1i$
0 1	$x_q = -1 + 1i$
1 0	$x_q = -1 - 1i$
1 1	$x_q = +1 - 1i$

Table 2.2 Example of the SM mapping process

Input Bits	Antenna Index	Transmit Symbol	Transmit Vector
0 0 0 0	$[0\ 0] \rightarrow j = 1$	$[0\ 0] \rightarrow x_q = +1 + 1i$	$[+1 + 1i \quad 0 \quad 0 \quad 0]$
0 0 0 1	$[0\ 0] \rightarrow j = 1$	$[0\ 1] \rightarrow x_q = -1 + 1i$	$[-1 + 1i \quad 0 \quad 0 \quad 0]$
0 0 1 0	$[0\ 0] \rightarrow j = 1$	$[1\ 0] \rightarrow x_q = -1 - 1i$	$[-1 - 1i \quad 0 \quad 0 \quad 0]$
0 0 1 1	$[0\ 0] \rightarrow j = 1$	$[1\ 1] \rightarrow x_q = +1 - 1i$	$[+1 - 1i \quad 0 \quad 0 \quad 0]$
0 1 0 0	$[0\ 1] \rightarrow j = 2$	$[0\ 0] \rightarrow x_q = +1 + 1i$	$[0 \quad +1 + 1i \quad 0 \quad 0]$
0 1 0 1	$[0\ 1] \rightarrow j = 2$	$[0\ 1] \rightarrow x_q = -1 + 1i$	$[0 \quad -1 + 1i \quad 0 \quad 0]$
0 1 1 0	$[0\ 1] \rightarrow j = 2$	$[1\ 0] \rightarrow x_q = -1 - 1i$	$[0 \quad -1 - 1i \quad 0 \quad 0]$
0 1 1 1	$[0\ 1] \rightarrow j = 2$	$[1\ 1] \rightarrow x_q = +1 - 1i$	$[0 \quad +1 - 1i \quad 0 \quad 0]$
1 0 0 0	$[1\ 0] \rightarrow j = 3$	$[0\ 0] \rightarrow x_q = +1 + 1i$	$[0 \quad 0 \quad +1 + 1i \quad 0]$
1 0 0 1	$[1\ 0] \rightarrow j = 3$	$[0\ 1] \rightarrow x_q = -1 + 1i$	$[0 \quad 0 \quad -1 + 1i \quad 0]$
1 0 1 0	$[1\ 0] \rightarrow j = 3$	$[1\ 0] \rightarrow x_q = -1 - 1i$	$[0 \quad 0 \quad -1 - 1i \quad 0]$
1 0 1 1	$[1\ 0] \rightarrow j = 3$	$[1\ 1] \rightarrow x_q = +1 - 1i$	$[0 \quad 0 \quad +1 - 1i \quad 0]$
1 1 0 0	$[1\ 1] \rightarrow j = 4$	$[0\ 0] \rightarrow x_q = +1 + 1i$	$[0 \quad 0 \quad 0 \quad +1 + 1i]$
1 1 0 1	$[1\ 1] \rightarrow j = 4$	$[0\ 1] \rightarrow x_q = -1 + 1i$	$[0 \quad 0 \quad 0 \quad -1 + 1i]$
1 1 1 0	$[1\ 1] \rightarrow j = 4$	$[1\ 0] \rightarrow x_q = -1 - 1i$	$[0 \quad 0 \quad 0 \quad -1 - 1i]$
1 1 1 1	$[1\ 1] \rightarrow j = 4$	$[1\ 1] \rightarrow x_q = +1 - 1i$	$[0 \quad 0 \quad 0 \quad +1 - 1i]$

Once mapped, the signal vector $\boldsymbol{x}_j$ is transmitted over the $N_R \times N_T$ MIMO channel, $\boldsymbol{H}$, and experiences N_R dimensional AWGN $\boldsymbol{n} = [n_1 \ n_2 \ \cdots \ n_{N_R}]^T$, where $\boldsymbol{H} = [\boldsymbol{h}_1 \ \boldsymbol{h}_2 \ \cdots \ \boldsymbol{h}_{N_T}]$.

The $N_R \times 1$ received signal vector is then given by [9, 12]:

$$\boldsymbol{y} = \sqrt{\rho}\boldsymbol{H}\boldsymbol{x}_j + \boldsymbol{n} \tag{2.2}$$

where ρ is the average SNR at each receive antenna, and both $\boldsymbol{H}$ and $\boldsymbol{n}$ have i.i.d entries, which follow the complex Gaussian distribution $CN(0,1)$.

Alternatively, if we assume that an arbitrary M-QAM symbol, x_q, is transmitted from the j^{th} transmit antenna, the received signal vector can be reduced and represented as [9, 12],

$$\boldsymbol{y} = \sqrt{\rho}\boldsymbol{h}_j x_q + \boldsymbol{n} \tag{2.3}$$

where $\boldsymbol{h}_j$ is a column vector which denotes the j^{th} column of $\boldsymbol{H}$, and $\boldsymbol{h}_j = [h_{1,j} \ h_{2,j} \ \cdots h_{N_R,j}]^T$.

2.2 SM Detection

SM employs an information symbol, as well as a transmit antenna index to encode data [12]. At the receiver, the SM detector obtains estimates of both the transmit antenna index and the information symbol. These estimates are then fed to the SM de-mapper so as to obtain an estimate of the original information bits [12]. The following subsections will detail both the sub-optimal [12] and optimal detection schemes [13] for SM.

2.2.1 Sub-optimal Detection

Mesleh *et. al*. [9, 12] first introduced the use of MRC at the receiver as a technique for detection. MRC was used as a detection algorithm to estimate the transmit antenna index, followed by the estimation of the transmitted symbol. In order to correctly estimate the transmit antenna index, the MRC algorithm assumed that the receiver had perfect knowledge of the channel [9, 12].

However, in [13] it was shown that the MRC algorithm proposed in [9, 12] was only valid under constrained channel conditions. Therefore, Jeganathan *et. al.* proposed a modified version of the MRC detection algorithm [13]. The modified detection rules can be applied under conventional channel conditions as follows [13],

$$z_j = \frac{\boldsymbol{h}_j^H \boldsymbol{y}}{\|\boldsymbol{h}_j\|_F} \tag{2.4}$$

where $j \in [1: N_T]$.

By using (2.4), the active transmit antenna index, $\hat{j}$, can be estimated as, [13]

$$\hat{j} = \underset{j}{\text{argmax}}(z_j) \tag{2.5}$$

Using the assumption that the estimate of the transmit antenna index is correct, the estimate of the transmit symbol, $\hat{x}_q$, can be obtained by applying the ML criterion [13]:

$$\hat{x}_q = \underset{q}{\text{argmin}} \left[\sqrt{\rho} \left\| \boldsymbol{h}_j x_q \right\|_F^2 - 2R\{\boldsymbol{h}_j^H \boldsymbol{y}\, x_q^*\} \right] \tag{2.6}$$

2.2.2 Optimal Detection

In [13], Jeganathan *et. al.* showed that using the MRC-based SM detector to decouple the estimation process of the transmit antenna index and symbol, resulted in reduced error performance. The ML-based detector proposed in [13] improved upon the sub-optimal MRC-based detection, and fully exploited the advantages of SM.

In contrast to sub-optimal SM detection, where the transmit antenna index is estimated prior to the transmit symbol, ML-based SM detection performs a joint detection of the transmit antenna index and transmit symbol.

Based on the ML principle, the active transmit antenna index and transmit symbol can be estimated as follows [13]:

$$[\hat{j}, \hat{x}] = \underset{j,q}{\text{argmin}} \left[\sqrt{\rho} \left\| \boldsymbol{h}_j x_q \right\|_F^2 - 2R\{\boldsymbol{y}^H \boldsymbol{h}_j x_q\} \right] \tag{2.7}$$

where $j \in [1: N_T]$, $q \in [1: M]$ and $\hat{j}$ and $\hat{x}$ represent the estimated transmit antenna index and estimated transmit symbol, respectively.

2.3 Analytical Performance Bounds for SM

The average BER of the optimal, ML-based SM detection scheme was evaluated in closed form in [13]. However, this theoretical performance bound was only applicable for binary phase shift keying (BPSK) modulation. As a result, Naidoo *et. al.* [14] derived a closed form expression to quantify the average BER performance of an arbitrary square M-QAM SM scheme.

The BER performance of SM is based on two estimation processes, viz. the estimation of the transmit antenna index and the estimation of the transmit symbol [9]. For the purpose of evaluating the BER, both processes are assumed to be independent [14].

The overall probability of error, P_e, is bound by [9, 14],

$$P_e \geq 1 - (1 - P_a)(1 - P_d) = P_a + P_d - P_a P_d \tag{2.8}$$

where P_a is the probability that the transmit antenna index is incorrect and P_d is the probability that the transmit symbol is incorrect.

In order to calculate the overall error probability, the error probability associated with each estimation process must be considered separately [14].

2.3.1 Analytical BER of Transmit Symbol Estimation

From [14], the probability that the transmit symbol is incorrect is approximated as,

$$P_d \cong \frac{SER(\rho)}{m} \tag{2.9}$$

where $m = \log_2 M$ is the number of bits per M-QAM symbol. $SER(\rho)$ is the average symbol error rate of a square M-QAM constellation, over i.i.d Rayleigh fading channels, and is calculated as [14]:

$$SER(\rho) = \frac{a}{c}\left\{\frac{1}{2}\left(\frac{2}{b\rho + 2}\right)^{N_R} - \frac{a}{2}\left(\frac{1}{b\rho + 1}\right)^{N_R} + (1 - a)\sum_{i=1}^{c-1}\alpha^{N_R} + \sum_{i=c}^{2c-1}\alpha^{N_R}\right\} \tag{2.10}$$

where $a = 1 - \frac{1}{\sqrt{M}}$, $b = \frac{3}{M-1}$, $\alpha = \frac{S_i}{b\rho + S_i}$, $S_i = 2\sin^2\theta_i$, $\theta_i = \frac{i\pi}{4c}$ and c is the number of summations, where $c > 10$ results in the converging of the simulated and theoretical SER [14].

2.3.2 Analytical BER of Transmit Antenna Index Estimation

Given that the transmit symbol index is perfectly estimated, the average BER of the transmit antenna index is union bounded by [14]:

$$P_a \leq \sum_{q=1}^{M} \sum_{j=1}^{N_T} \sum_{\hat{j}=1}^{N_T} \frac{N(j,\hat{j})\, P(x_j \to x_{\hat{j}})}{N_T M} \tag{2.11}$$

where $P(x_j \to x_{\hat{j}})$ denotes the PEP of choosing signal vector $x_{\hat{j}}$, given that x_j was transmitted and $N(j,\hat{j})$ is the number of bits in error between the transmit antenna index j, and the estimated transmit antenna index $\hat{j}$.

The closed form solution of the PEP is given as [14],

$$P(x_j \to x_{\hat{j}}) = \mu_\alpha^{N_R} \sum_{z=0}^{N_R-1} \binom{N_R - 1 + z}{z} (1 - \mu_\alpha)^z \tag{2.12}$$

where $\mu_\alpha = \frac{1}{2}\left(1 - \sqrt{\frac{\sigma_\alpha^2}{1+\sigma_\alpha^2}}\right)$ and $\sigma_\alpha^2 = \frac{\rho}{2}|x_q|^2$.

2.4 Computational Complexity Analysis at the Receiver

The computational complexity of the aforementioned optimal and sub-optimal SM detection schemes were calculated in terms of the number of flops.

2.4.1 Sub-optimal Detection

As previously mentioned, the sub-optimal SM detection scheme comprises of two estimation processes, viz. transmit antenna and symbol estimation. The complexity associated with transmit antenna detection is based on (2.4), which must be calculated for the N_T column vectors in $\boldsymbol{H}$. The numerator requires $2N_R$ flops, whilst N_R flops are imposed by the denominator. Therefore, the computational complexity associated with transmit antenna detection is,

$$\delta_{antenna} = (3N_R + 1)N_T \tag{2.13}$$

The complexity of the symbol detection is imposed by (2.6). The first term of (2.6) imposes $3N_R$ flops, whilst the second term requires $4N_R$ flops. Taking into account the subtraction of second term from the first term, the complexity of the symbol estimation is,

$$\delta_{symbol} = (7N_R + 1)M \tag{2.14}$$

Therefore, the total computational complexity of the sub-optimal, MRC-based, SM detection is given by,

$$\delta_{sub-opt} = (3N_R + 1)N_T + (7N_R + 1)M \tag{2.15}$$

2.4.2 Optimal Detection

The computational complexity of the optimal SM detector is rendered by analysing the ML-based detection rule given in (2.7). ML-based detection requires an exhaustive search. As a result, (2.7) must be calculated for each of the M symbols, as well as for each of the N_T antenna indices. When analysing the first term of (2.7), $\left\|\boldsymbol{h}_j x_q\right\|_F^2$ requires $3N_R - 1$ flops. Therefore, the computational complexity imposed by $\sqrt{\rho}\left\|\boldsymbol{h}_j x_q\right\|_F^2$ is,

$$\delta_{term\,1} = 3N_R \tag{2.16}$$

Similarly, the number of flops required for the execution of the second term is,

$$\delta_{term\,2} = 4N_R \tag{2.17}$$

Since term 2 is subtracted from term 1, the total computational complexity imposed by the ML-based SM detector is,

$$\delta_{opt} = (7N_R + 1)MN_T \tag{2.18}$$

2.5 Simulation Results and Discussion

In this section, Monte Carlo simulation results for various SM configurations have been presented. For each configuration, the simulation results plot the average BER performance against the average SNR at each receive antenna. Furthermore, these results are compared to the analytical performance bounds detailed in (2.8) – (2.12).

It has been assumed that all Monte Carlo simulations are performed over an i.i.d Rayleigh flat fading channel with AWGN. Gray-coded M-QAM constellations have been utilised for all simulations. Additionally, it is assumed that the receiver has full knowledge of the channel. The Monte Carlo simulations are depicted for spectral efficiencies of 4, 6 and 8 b/s/Hz. This ensures the consideration of a wide variety of hardware configurations for SM. The notation used to denote the $N_T \times N_R$ configuration of SM is (M, N_T, N_R).

Figure 2.2 shows the BER performance of Gray-coded 4-QAM SM, using optimal detection. The results have depicted 4×4 and 4×2 4-QAM SM, with each configuration being analytically compared to the performance bounds presented in Section 2.3.

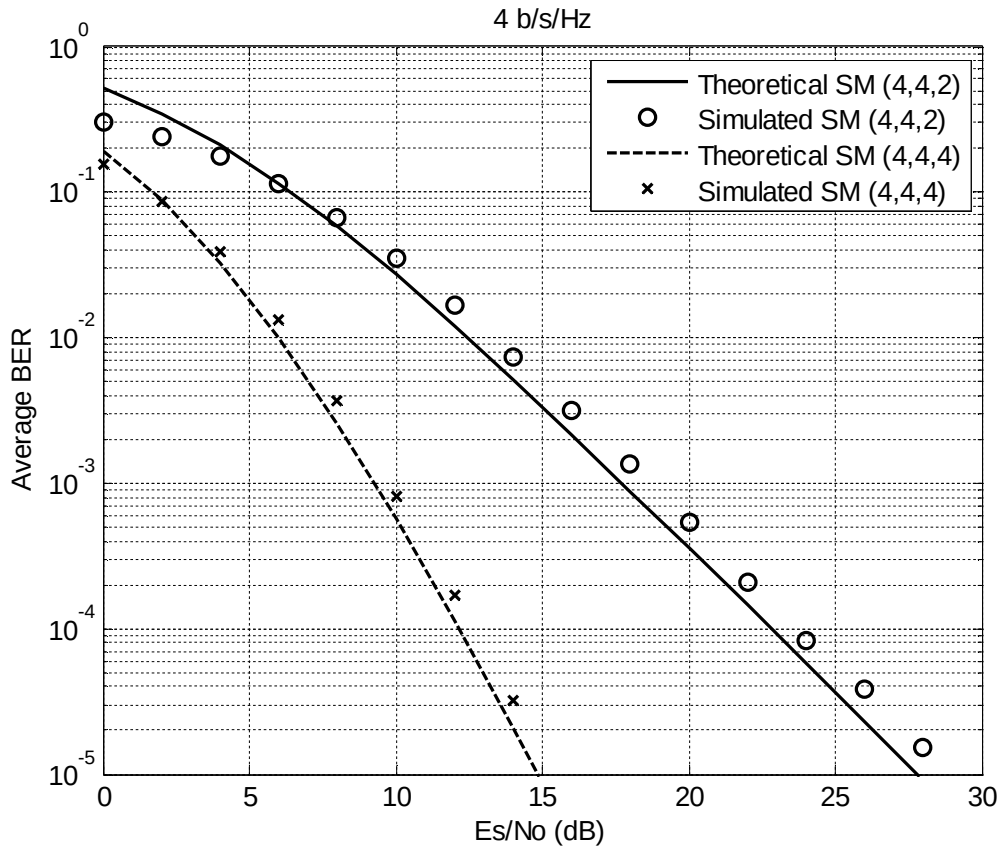

Figure 2.2 BER performance of 4-QAM SM

For Figure 2.2, at a BER of 10^{-5}, the 4×4 4-QAM SM scheme shows a gain of approximately 11 dB over the 4×2 4-QAM SM configuration. As can be seen, and as expected, the BER performance of SM improves as the number of receive antenna increases. Furthermore, it is noted that by increasing the number of receive antennas, the analytical bound and Monte Carlo simulations are more closely matched.

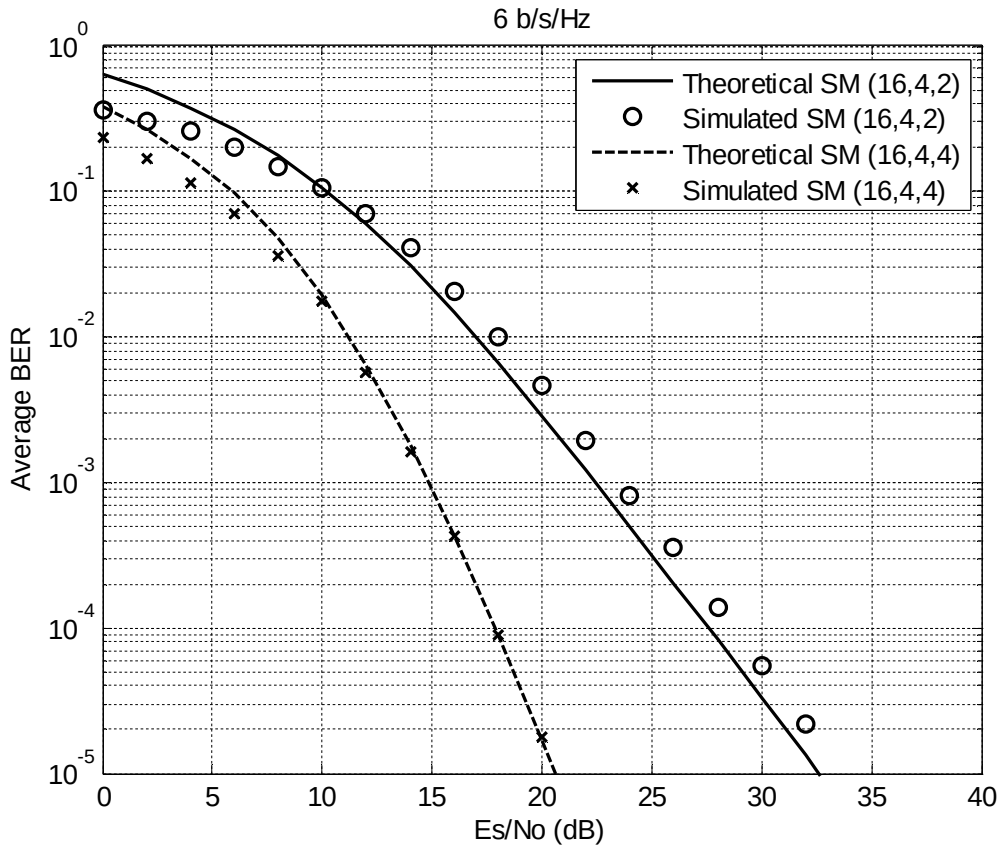

Figure 2.3 BER performance of 16-QAM SM

Figure 2.3 and Figure 2.4 depict the BER performance of 16-QAM and 64-QAM SM, respectively. Figure 2.3 depicts two configurations of SM, viz. 4×2 16-QAM and 4×4 16-QAM. As previously noted, an increase in the number of receive antennas has improved the BER performance. Furthermore, the analytical results closely match the results produced by the Monte Carlo simulations.

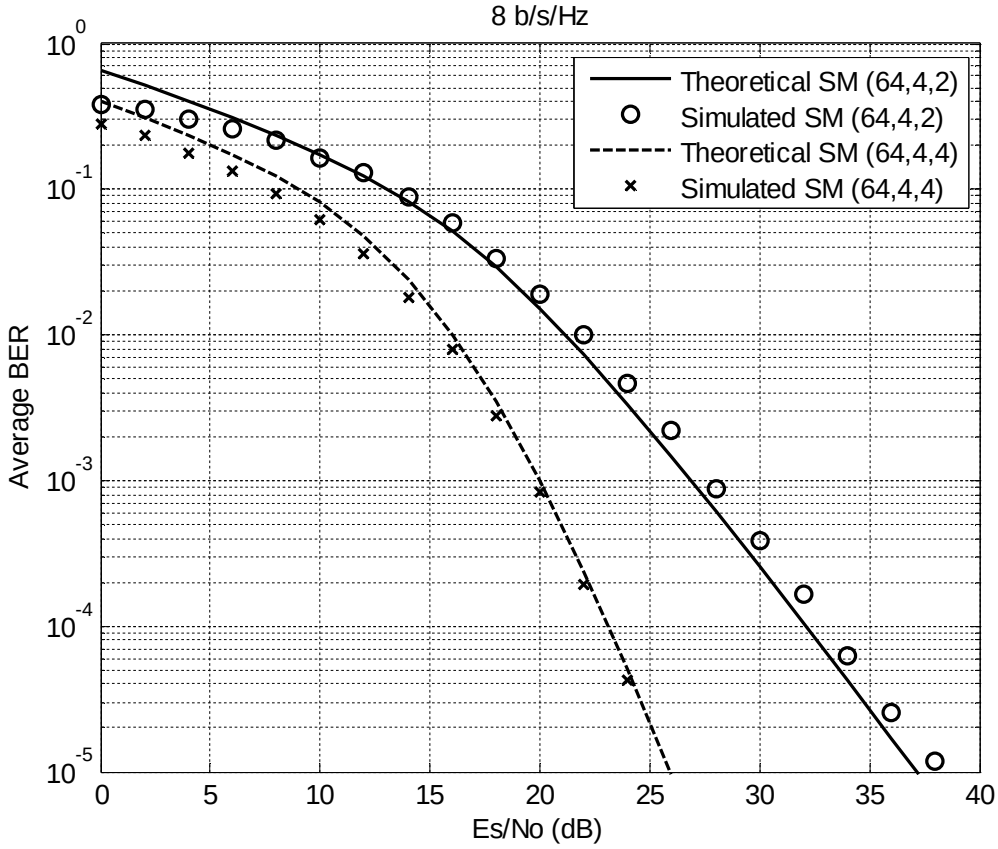

Figure 2.4 BER performance of 64-QAM SM

Figure 2.4 illustrates the BER performance of Gray-coded 64-QAM SM for a 4×2 and 4×4 MIMO configuration. Similarly to prior SM configurations, the analytical performance bounds closely match the Monte Carlo simulations for SM.

As previously mentioned, SM was introduced as an innovative, spectrally efficient, MIMO scheme, which was capable of improving upon the error performance achieved by prior MIMO schemes. The results documented in Section 2 have verified that SM is a viable MIMO system, which proves to be beneficial in wireless communications.

3 QUADRATURE SPATIAL MODULATION

Although SM has been presented as a highly beneficial MIMO scheme, room for improvement still exists. QSM was proposed by Mesleh *et. al.* [30, 31] as an innovative way of improving upon the spectral efficiency of SM. This chapter introduces the key concepts behind QSM, as well as provides a derivation of the analytical performance of QSM. Furthermore, Section 3.3 discusses the BER performance of QSM, as compared to SM.

3.1 System Model

Consider the QSM scheme, depicted in Figure 3.1, with N_T transmit antennas and N_R receive antennas.

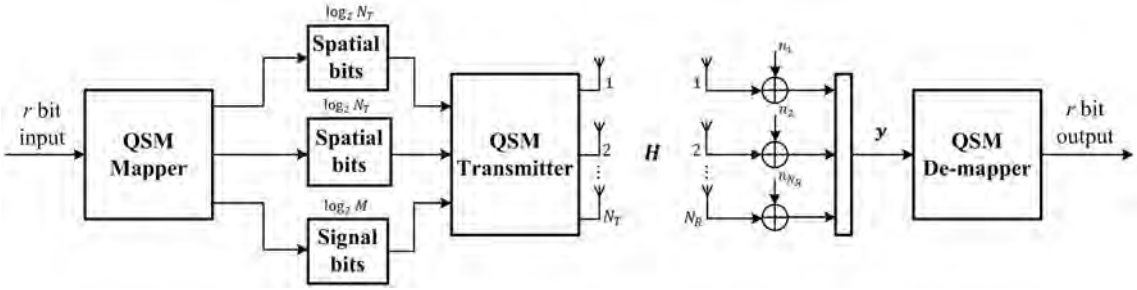

Figure 3.1 QSM System Model [30, 31]

The number of bits that can be transmitted using QSM is given as follows [30, 31]:

$$r = \log_2(MN_T{}^2) \tag{3.1}$$

where, as earlier, M denotes the modulation order of M-QAM.

The incoming data bits are split into three groups: The first $\log_2 M$ bits modulates a signal constellation symbol x_q, where $q \in [1: M]$, and the remaining $2\log_2 N_T$ bits modulates two separate spatial constellation symbols [30, 31]. The symbol x_q is then decomposed into its real and imaginary parts, denoted by x_q^R and x_q^I, respectively. Therefore, the active transmit antennas that transmit x_q^R and x_q^I corresponds to l_R and l_I, respectively [30, 31]. As mentioned in Section 2.1, unlike QSM, SM is limited to the use of a single active transmit antenna. SM uses the active transmit antenna, j, to transmit the constellation symbol x_q. However, QSM uses up to two active transmit antennas, thereby showing an enhancement in spectral efficiency.

The Gray-coded constellation points used for 4-QAM has been previously shown in Table 2.1, whilst the Gray-coded constellation points used for 16-QAM is shown in Table 3.1.

Table 3.1 Gray-coded constellation points for 16-QAM

$\log_2 M$ bits	M-QAM Symbol
0 0 0 0	$x_q = -3 + 3i$
0 0 0 1	$x_q = -3 + 1i$
0 0 1 0	$x_q = -3 - 3i$
0 0 1 1	$x_q = -3 - 1i$
0 1 0 0	$x_q = -1 + 3i$
0 1 0 1	$x_q = -1 + 1i$
0 1 1 0	$x_q = -1 - 3i$
0 1 1 1	$x_q = -1 - 1i$
1 0 0 0	$x_q = +3 + 3i$
1 0 0 1	$x_q = +3 + 1i$
1 0 1 0	$x_q = +3 - 3i$
1 0 1 1	$x_q = +3 - 1i$
1 1 0 0	$x_q = +1 + 3i$
1 1 0 1	$x_q = +1 + 1i$
1 1 1 0	$x_q = +1 - 3i$
1 1 1 1	$x_q = +1 - 1i$

Using the constellation points provided in Table 2.1 and Table 3.1, various examples of the mapping technique for QSM is shown in Table 3.2. The examples shown in Table 3.2 illustrate the mapping technique for QSM for selected 4-QAM and 16-QAM configurations.

Table 3.2 Example mapping for QSM for selected M-QAM configurations

Configuration	$r = \log_2(MN_T^2)$ Input Bits	First $\log_2 M$ bits	Second $\log_2 N_T$ bits	Third $\log_2 N_T$ bits
M = 4, N_T = 2, N_R = 4	0 1 0 1	$\log_2 4$ = 2 bits ⇒ [0 0] $x_q = -1 + 1i$ $x_q^R = 1$ $x_q^I = +1i$	$\log_2 2$ = 1 bit ⇒ [0] $l_R = 1$	$\log_2 2$ = 1 bit ⇒ [1] $l_I = 2$
M = 4, N_T = 4, N_R = 4	1 1 0 1 1 0	$\log_2 4$ = 2 bits ⇒ [1 1] $x_q = +1 - 1i$ $x_q^R = 1$ $x_q^I = -1i$	$\log_2 4$ = 2 bits ⇒ [0 1] $l_R = 2$	$\log_2 4$ = 2 bits ⇒ [1 0] $l_I = 3$
M = 16, N_T = 4, N_R = 4	1 0 0 1 1 1 1 1	$\log_2 4$ = 2 bits ⇒ [1 0 0 1] $x_q = +3 + 1i$ $x_q^R = 3$ $x_q^I = +1i$	$\log_2 4$ = 2 bits ⇒ [1 1] $l_R = 4$	$\log_2 4$ = 2 bits ⇒ [1 1] $l_I = 4$

The $N_R \times 1$ received signal vector is defined as [30, 31]:

$$\boldsymbol{y} = \sqrt{\rho/\mu}\left(\boldsymbol{h}_{l_R} x_q^R + i\boldsymbol{h}_{l_I} x_q^I\right) + \boldsymbol{n} \tag{3.2}$$

where $\mu = \begin{cases} 1, & l_R = l_I \\ 2, & l_R \neq l_I \end{cases}$, $\rho = \frac{E_S}{N_0}$ is the average SNR at each receive antenna, E_S denotes the energy per transmitted symbol, and N_0 is the single-sided power spectral density. $\boldsymbol{H}$ is an $N_R \times N_T$ complex channel gain matrix with i.i.d entries with distribution $CN(0,1)$. $\boldsymbol{h}_{l_R}$ and $\boldsymbol{h}_{l_I}$ represent the l_R^{th} and l_I^{th} column of $\boldsymbol{H}$, respectively. $\boldsymbol{n}$ represents an $N_R \times 1$ complex AWGN vector with $CN(0,1)$ i.i.d entries. Note that x_q^R and x_q^I are from the M-QAM set, and have been mapped using Gray-coded constellation points.

The optimum ML detector for QSM is defined in [30, 31] as,

$$\left[\hat{l}_R, \hat{l}_I, \hat{x}_q^R, \hat{x}_q^I\right] = \underset{l_R, l_I, x_q^R, x_I^q}{\operatorname{argmin}} \left\| \boldsymbol{y} - \sqrt{\rho/\mu}\left(\boldsymbol{h}_{l_R} x_q^R + i\boldsymbol{h}_{l_I} x_q^I\right) \right\|_F^2 \tag{3.3}$$

$$= \underset{l_R, l_I, x_q^R, x_I^q}{\operatorname{argmin}} \{\|\boldsymbol{g}\|_F^2 - 2R\{\boldsymbol{y}^H \boldsymbol{g}\}\}$$

where $\boldsymbol{g} = \sqrt{\rho/\mu}\left(\boldsymbol{h}_{l_R} x_q^R + i\boldsymbol{h}_{l_I} x_q^I\right)$, $\hat{l}_R$ and $\hat{l}_I$ are the detected antenna indices and $\hat{x}_q^R$ and $\hat{x}_q^I$ are the detected data symbols.

3.2 Analytical Performance of Quadrature Spatial Modulation

In [28, 29], a method to compute the average BER of the QSM scheme was derived. The BER of the QSM scheme was derived in [30, 31], and is given as:

$$P_b = \frac{1}{2^r} \sum_{l=1}^{2^r} \sum_{k=1}^{2^r} \frac{1}{r} \bar{P}_e\left(\boldsymbol{g}_l \to \boldsymbol{g}_k\right) N(l,k) \tag{3.4}$$

where $\bar{P}_e$ is the average PEP and $N(l,k)$ is the number of bit errors associated with the corresponding PEP event.

The average PEP is calculated in [30, 31] as:

$$\overline{P_e}\left(\boldsymbol{g}_l \rightarrow \boldsymbol{g}_k\right) = \frac{1}{2}\left(1 - \sqrt{\frac{\bar{\beta}/_2}{1 + \bar{\beta}/_2}}\right) \tag{3.5}$$

where $\bar{\beta}$ is given as:

$$\bar{\beta} = \begin{cases} \gamma\left(\left|x_q^R\right|^2 + \left|\hat{x}_q^R\right|^2 + \left|x_q^I\right|^2 + \left|\hat{x}_q^I\right|^2\right) \text{ if } \boldsymbol{h}_{l_R} \neq \widehat{\boldsymbol{h}}_{l_R} \text{ and } \boldsymbol{h}_{l_I} \neq \widehat{\boldsymbol{h}}_{l_I} \\ \gamma\left(\left|x_q^R - \hat{x}_q^R\right|^2 + \left|x_q^I\right|^2 + \left|\hat{x}_q^I\right|^2\right) \text{ if } \boldsymbol{h}_{l_R} = \widehat{\boldsymbol{h}}_{l_R} \text{ and } \boldsymbol{h}_{l_I} \neq \widehat{\boldsymbol{h}}_{l_I} \\ \gamma\left(\left|x_q^R\right|^2 + \left|\hat{x}_q^R\right|^2 + \left|x_q^I - \hat{x}_q^I\right|^2\right) \text{ if } \boldsymbol{h}_{l_R} \neq \widehat{\boldsymbol{h}}_{l_R} \text{ and } \boldsymbol{h}_{l_I} = \widehat{\boldsymbol{h}}_{l_I} \\ \gamma\left(\left|x_q^R - \hat{x}_q^R\right|^2 + \left|x_q^I - \hat{x}_q^I\right|^2\right) \text{ if } \boldsymbol{h}_{l_R} = \widehat{\boldsymbol{h}}_{l_R} \text{ and } \boldsymbol{h}_{l_I} = \widehat{\boldsymbol{h}}_{l_I} \end{cases} \tag{3.6}$$

and $\gamma = \frac{\rho}{2}$.

3.3 Simulation Results and Discussion

In this section, analytical and Monte Carlo simulation results are presented for the QSM scheme. For all schemes, the analytical performance of QSM has been compared to the Monte Carlo simulations using (3.4) and (3.5). Furthermore, the error performance of QSM has also been compared to Monte Carlo simulations of SM. In order to validate the Monte Carlo simulations for QSM against existing literature, the average BER was plotted against the average SNR per symbol for spectral efficiencies of 4, 6 and 8 b/s/Hz. Furthermore, it is assumed that the channel information is perfectly known at the receiver.

The notation used to denote the configuration of QSM and SM is (M, N_T, N_R).

In Figure 3.2, Monte Carlo simulations for a QSM system with 4-QAM modulation and a spectral efficiency of 4 b/s/Hz are illustrated. The upper-bound analytical results for QSM are also shown.

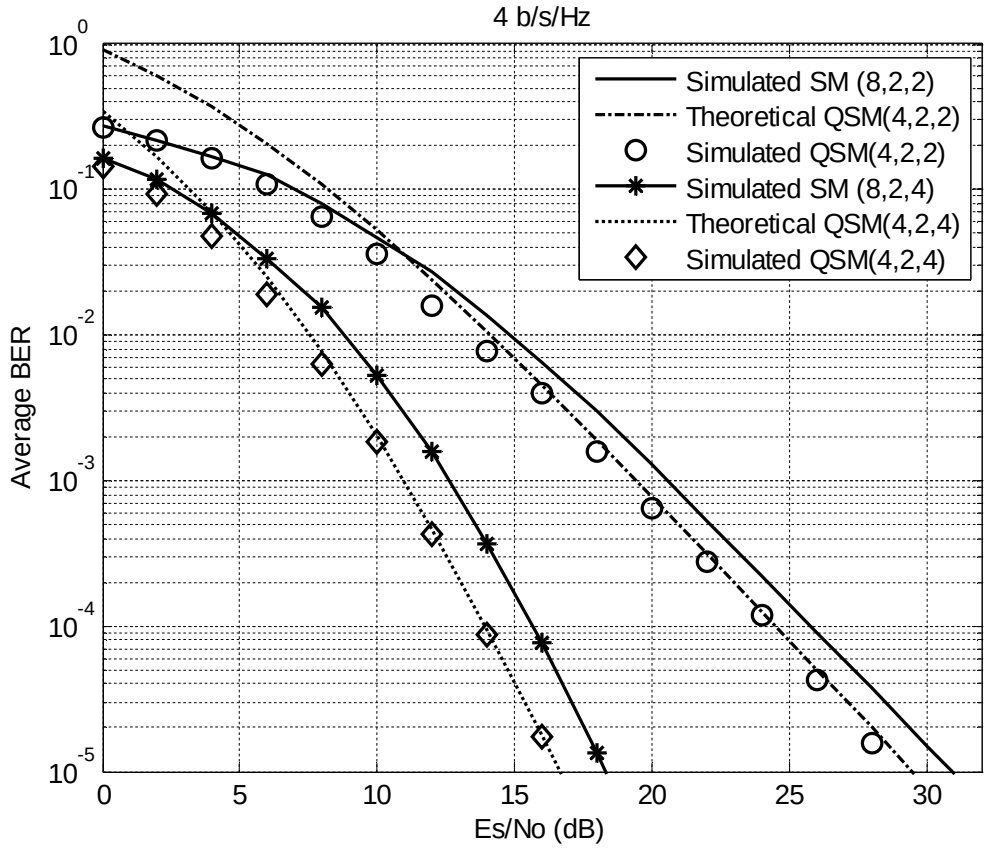

Figure 3.2 BER performance of QSM for 4 b/s/Hz

For 2×2 and 2×4 4-QAM QSM, theoretical and simulated results match closely, especially at high SNR values. In addition, it is observed that the performance of QSM exceeds that of conventional SM. For example, at a BER of 10^{-5}, the 2×4 4-QAM QSM scheme has an SNR gain of approximately 1.94 dB over the 2×4 8-QAM SM scheme, whilst 2×2 4-QAM QSM has an SNR gain of 1.67 dB over the 2×2 8-QAM SM scheme. Furthermore, increasing the number of receive antennas for QSM, from $N_R = 2$ to $N_R = 4$, results in a significant improvement in error performance. When $N_R = 4$, QSM attains an approximate SNR gain of 12.50 dB over QSM with $N_R = 2$.

By processing the constellation symbol prior to transmission, QSM is able to achieve significant SNR gains compared to SM. Furthermore, by increasing the number of active transmit antennas in each transmission, QSM further improves upon the spectral efficiency of SM.

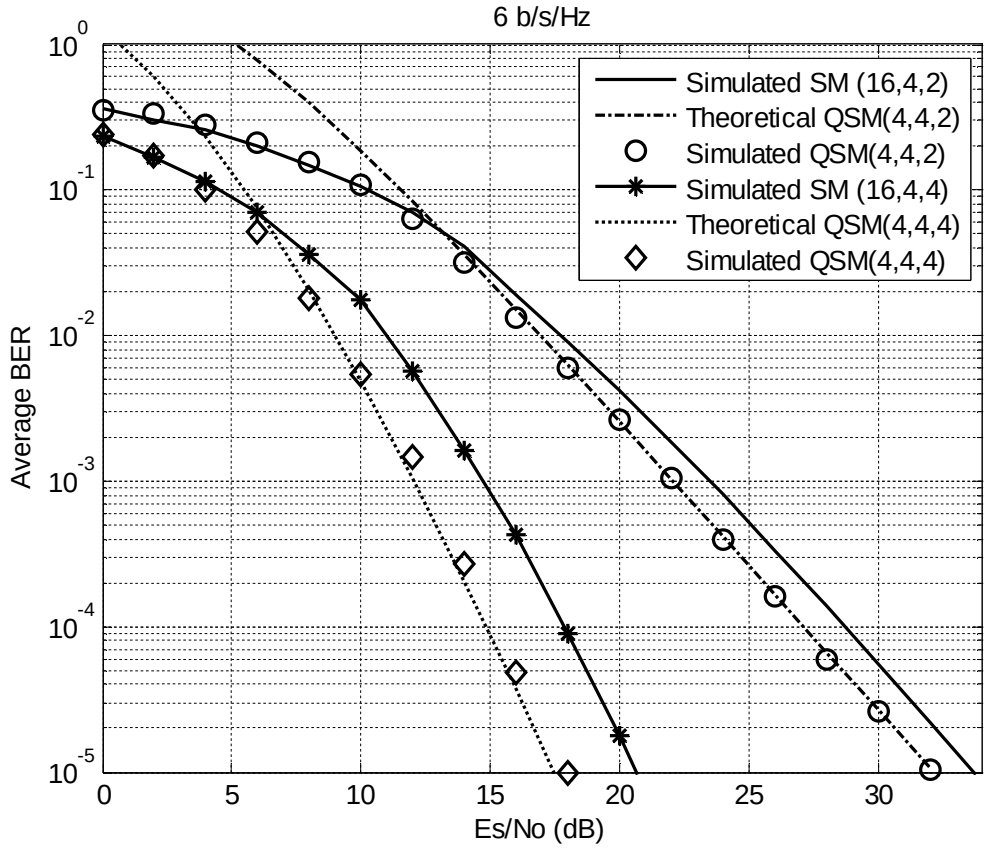

Figure 3.3 BER performance of QSM for 6 b/s/Hz

Figure 3.3 depicts a 4×2 and 4×4 QSM system, with 4-QAM modulation, and a spectral efficiency of 6 b/s/Hz. Once again, the simulated and analytical results for QSM match closely in both configurations, and the error performance of QSM surpasses that of conventional SM. Analysing the error performance of 4×4 4-QAM QSM and 4×4 16-QAM SM, at a BER of 10^{-5}, QSM has an SNR gain of approximately 2.94 dB as compared to SM. Similarly, comparing 4×2 4-QAM QSM to 4×2 16-QAM SM, QSM results in a 1.47 dB SNR gain over SM. The 4×4 QSM system has a 13.54 dB SNR gain over the 4×2 QSM configuration.

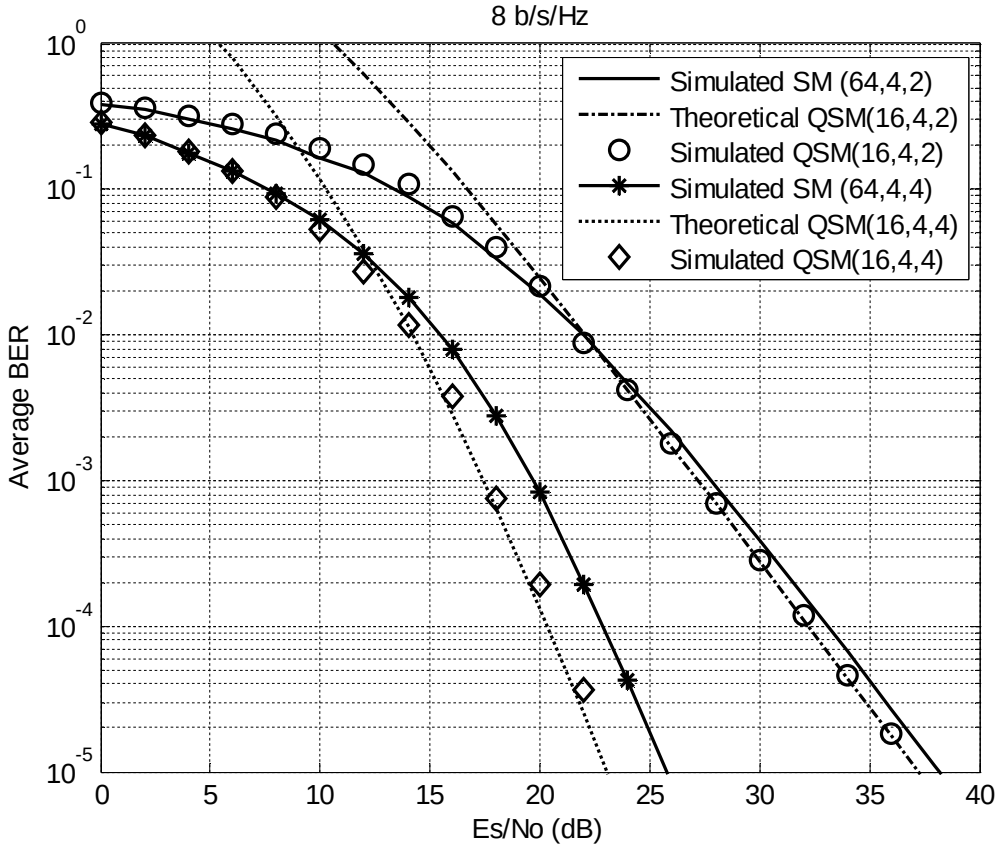

Figure 3.4 BER performance of QSM for 8 b/s/Hz

In keeping with the results presented in Figure 3.2 and Figure 3.3, Figure 3.4 verifies that QSM outperforms SM. It is also noted that increasing the number of receive antennas continues to improve BER performance. At a BER of 10^{-5}, the 4×4 16-QAM QSM system shows a 2.33 dB SNR gain over 4×4 64-QAM SM scheme. At the same time, 4×2 16-QAM QSM exhibits a 1.17 dB gain as compared to the 4×2 64-QAM SM configuration.

To conclude the findings of this chapter, the SNR gains realised by QSM, with respect to SM, has been tabulated in Table 3.3. For each configuration of QSM presented in the above simulations, the SNR gain achieved by QSM is documented below. As can be seen, it has been proven that QSM improves both the BER performance and spectral efficiency of SM.

Table 3.3 Summary of SNR gain (dB) of QSM, with respect to SM

Configuration	$M = 4, N_T = 2$	$M = 4, N_T = 4$	$M = 16, N_T = 4$
$N_R = 2$	1.67	1.47	1.17
$N_R = 4$	1.94	2.94	2.33

4 TRANSMIT ANTENNA SELECTION FOR QUADRATURE SPATIAL MODULATION

QSM has been proven to be an attractive MIMO scheme, which improves the spectral efficiency of SM, whilst simultaneously reduces its BER performance. However, as discussed in Section 1.1.3, one promising method of increasing the transmit diversity and improving the BER performance of SM, was to employ the use of TAS. Motivated by this, this chapter applies several TAS algorithms to QSM. In the sub-sections to follow, these algorithms are categorised as either optimal or sub-optimal. The use of optimal TAS has been extensively documented in literature, with its most prominent drawback being the extremely high computational complexity it imposes. Consequently, the implementation of low-complexity, sub-optimal TAS techniques has since proved to be a topic of great interest.

Figure 4.1 depicts the combination of QSM with TAS, where it is assumed that there exists N_{TOTAL} transmit antenna elements and N_R receive antenna elements.

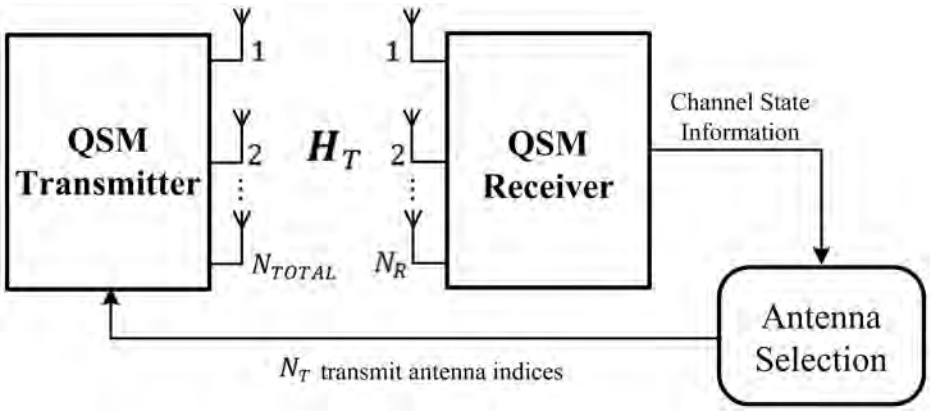

Figure 4.1 System model of QSM with TAS [42, 43]

The $N_R \times N_{TOTAL}$ complex channel gain matrix is given by $\boldsymbol{H}_T$. Based on the channel matrix $\boldsymbol{H}_T$, and the chosen antenna selection technique, a set of N_T transmit antennas are selected, where $N_T < N_{TOTAL}$. The indices of the selected N_T transmit antennas are sent to the QSM transmitter to be utilised in conventional QSM. For QSM, the real part of the symbol is transmitted on the first antenna index, and the imaginary part of the symbol is transmitted on a second antenna index. Hence, for QSM, $N_T \geq 2$.

Each TAS algorithm has been presented in detail, along with the computational complexity imposed by the said algorithm. The computational complexity imposed by each TAS scheme has been calculated in terms of the number of flops, where a flop constitutes an addition, subtraction, multiplication or division.

4.1 Optimal Transmit Antenna Selection

Optimal TAS refers to a selection criterion, which when compared to alternate TAS algorithms, yields the best error performance.

4.1.1 Euclidean-Distance based Antenna Selection for QSM

The use of ED as a selection criterion for TAS was first proposed by Yang *et. al*. [32, 33]. By selecting the subset of transmit antennas, which maximises the minimum ED between all transmit vectors, one can ensure that optimal error performance is obtained. ED based antenna selection for QSM (EDAS-QSM) is based on this key concept.

As shown previously, the $N_R \times 1$ QSM received signal is given by:

$$\boldsymbol{y} = \sqrt{\rho/\mu}\left(\boldsymbol{h}_{l_R} x_q^R + i\boldsymbol{h}_{l_I} x_q^I\right) + \boldsymbol{n}$$

$$\mu = \begin{cases} 1, & l_R = l_I \\ 2, & l_R \neq l_I \end{cases}$$

Much like SM, the average BER of QSM does not have a closed-form solution. In order to approximate the average BER of SM, Yang *et. al.* [26] employed the nearest neighbour approximation. Similarly to [24], by using the nearest neighbour approximation, the PEP of QSM for a given channel $\boldsymbol{H}$ is:

$$P_e \cong \lambda \cdot Q\left(\sqrt{\rho/\mu\, \mathrm{d}_{min}^2(\boldsymbol{H})}\right) \tag{4.1}$$

where λ denotes the number of neighbour points, $Q(\cdot)$ is the Gaussian Q-function, defined as $Q(x) = \frac{1}{\sqrt{2\pi}}\int_x^\infty e^{\frac{-t^2}{2}} dt$ and $\mathrm{d}_{min}^2(\boldsymbol{H})$ is the minimum squared ED between a pair of symbols, given as $\min_{x_q \neq \hat{x}_q} \left\| \boldsymbol{h}_{l_R} x_q^R + i\boldsymbol{h}_{l_I} x_q^I - \widehat{\boldsymbol{h}}_{l_R} \hat{x}_q^R - i\widehat{\boldsymbol{h}}_{l_I} \hat{x}_q^I \right\|_F^2$.

From (4.1) it can be seen that in order to minimise the error performance of the system, the minimum ED must be maximised, i.e. the argument of the Q-function can be maximised by adjusting the transmit parameters of $\mathsf{d}_{min}^2(\boldsymbol{H})$.

The steps followed in order to execute the EDAS-QSM algorithm are detailed below.

Step 1: N_S represents the total number of possible transmit antenna subset combinations, where $N_S = \binom{N_{TOTAL}}{N_T}$.

Step 2: The transmit antenna subset that maximises the minimum ED among all transmit antennas is given by:

$$l_{selected} = \underset{l \,\epsilon\, [1:N_S]}{\operatorname{argmax}} \left(\min_{\substack{x_q, \hat{x}_q \in \tau \\ x_q \neq \hat{x}_q}} \left\| \boldsymbol{h}_{l_R} x_q^R + i\boldsymbol{h}_{l_I} x_q^I - \widehat{\boldsymbol{h}}_{l_R} \hat{x}_q^R - i\widehat{\boldsymbol{h}}_{l_I} \hat{x}_q^I \right\|_F^2 \right) \tag{4.2}$$

where $l_{selected}$ represents the optimal antenna subset and τ is the set of all possible transmit symbols.

4.1.1.1 Analysis of Computational Complexity for EDAS-QSM

The computational complexity of each TAS algorithm has been formulated using the floating point operation approach of [45]. Table 4.1 summarises the required flops associated with various common operations, such as addition, multiplication, subtraction and the Frobenius norm operation.

Table 4.1 Summary of the number of flops required for various operations

Operation	Required Number of Flops
$a_1 + a_2 + \cdots + a_n$	$(n-1)$
$a_1 - a_2 - \cdots - a_n$	$(n-1)$
$a_1 \times a_2 \times \ldots \times a_n$	(n)
$\|\boldsymbol{A}\|_F^2 \;\; (\boldsymbol{A} \in \mathbb{C}^{L \times 1})$	$(2L-1)$

The computational complexity of EDAS-QSM is imposed by (4.2), where it is required to solve $\min_{\substack{x_q,\hat{x}_q\in\tau \\ x_q\neq\hat{x}_q}} \left\| \boldsymbol{h}_{l_R} x_q^R + i\boldsymbol{h}_{l_I} x_q^I - \widehat{\boldsymbol{h}}_{l_R} \hat{x}_q^R - i\widehat{\boldsymbol{h}}_{l_I} \hat{x}_q^I \right\|_F^2$ for all symbol combinations, as well as for all combinations of transmit antenna indices.

The computational complexity imposed by solving $\left\| \boldsymbol{h}_{l_R} x_q^R + i\boldsymbol{h}_{l_I} x_q^I - \widehat{\boldsymbol{h}}_{l_R} \hat{x}_q^R - i\widehat{\boldsymbol{h}}_{l_I} \hat{x}_q^I \right\|_F^2$ can be broken down as follows: $(2N_R - 1)$ flops are required to compute the squared Frobenius norm operation. Additionally, there are 4 multiplications, 1 addition and 2 subtractions which take place within the Frobenius norm operation. Therefore, the number of flops required to compute $\left\| \boldsymbol{h}_{l_R} x_q^R + i\boldsymbol{h}_{l_I} x_q^I - \widehat{\boldsymbol{h}}_{l_R} \hat{x}_q^R - i\widehat{\boldsymbol{h}}_{l_I} \hat{x}_q^I \right\|_F^2$ is $(9N_R - 1)$.

An exhaustive search of (4.2) requires that the ED be calculated for all symbol combinations of x_q and $\hat{x}_q$, such that $x_q \neq \hat{x}_q$. This requires $4M(4M - 1)(9N_R - 1)$ flops. EDAS-QSM must then be executed for each of the N_S transmit antenna subsets. In accordance with QSM, EDAS-QSM must be performed for each antenna pair within each antenna subset, i.e. EDAS-QSM must be executed a total of $\binom{N_T}{2} \times N_S$ times. Therefore, the computational complexity of EDAS-QSM is:

$$\delta_{EDAS-QSM} = 4M(4M - 1)(9N_R - 1)\binom{N_T}{2}\binom{N_{TOTAL}}{N_T} \tag{4.3}$$

Through the use of Monte Carlo simulations, it is verified that EDAS-QSM provides superior error performance. However, the computational complexity involved in executing EDAS-QSM is unfeasibly high. For example, a 16-QAM 8×4 QSM system with $N_{TOTAL} = 10$, would require 117,811,200 flops to be completed. This level of complexity makes real-world implementation unrealistic. It is for this reason that reducing the complexity of EDAS-QSM, whilst maintaining system performance, is of paramount importance.

4.1.2 Reduced-Complexity Euclidean-Distance based Antenna Selection

Despite yielding optimal error performance, EDAS suffers from practical limitations due to the high computational complexity imposed by direct computation of the scheme. On this note, [39, 41] proposed a low-complexity computational algorithm for EDAS-SM, which reduced computational complexity, whilst maintaining the error performance of the original EDAS technique. In this sub-section, an algorithm for efficient computation of EDAS-QSM is proposed, i.e. RCEDAS-QSM.

For EDAS-QSM, the ED between each symbol was calculated for all possible combinations of $(\boldsymbol{h}_{l_R}, \widehat{\boldsymbol{h}}_{l_R})$ and $(\boldsymbol{h}_{l_I}, \widehat{\boldsymbol{h}}_{l_I})$, where $\boldsymbol{h}_{l_R}$ and $\boldsymbol{h}_{l_I}$ are the vectors that were transmitted, and $\widehat{\boldsymbol{h}}_{l_R}$ and $\widehat{\boldsymbol{h}}_{l_I}$ are the vectors which were received. This search was exhaustive, and the accompanying computational complexity was extremely high. When calculating the ED between a symbol pair, several combinations of $(\boldsymbol{h}_{l_R}, \widehat{\boldsymbol{h}}_{l_R})$ and $(\boldsymbol{h}_{l_I}, \widehat{\boldsymbol{h}}_{l_I})$ were found to be repeated. As a result, the ED was unnecessarily calculated, and this contributed to the excessive complexity of EDAS-QSM.

Consider a scenario in which $N_{TOTAL} = 3$ and $N_T = 2$. Using EDAS-QSM, the possible combinations of $(\boldsymbol{h}_{l_R}, \widehat{\boldsymbol{h}}_{l_R})$ and $(\boldsymbol{h}_{l_I}, \widehat{\boldsymbol{h}}_{l_I})$ can then be represented by the following matrices:

$$(\boldsymbol{h}_{l_R}, \widehat{\boldsymbol{h}}_{l_R}) = \begin{pmatrix} (1,1) & (1,2) & (1,3) \\ (2,1) & (2,2) & (2,3) \\ (3,1) & (3,2) & (3,3) \end{pmatrix}$$

$$(\boldsymbol{h}_{l_I}, \widehat{\boldsymbol{h}}_{l_I}) = \begin{pmatrix} (1,1) & (1,2) & (1,3) \\ (2,1) & (2,2) & (2,3) \\ (3,1) & (3,2) & (3,3) \end{pmatrix}$$

Upon analysis of the combinations of $\boldsymbol{h}_{l_R}$ and $\widehat{\boldsymbol{h}}_{l_R}$, one can clearly see that many of these combinations have been repeated, e.g. $(1,2)$ and $(2,1)$, $(2,3)$ and $(3,2)$, and $(1,3)$ and $(3,1)$. A similar repetitiveness can also be seen in the combinations of $\boldsymbol{h}_{l_I}$ and $\widehat{\boldsymbol{h}}_{l_I}$. Since the ED between each symbol was calculated for all combinations of $(\boldsymbol{h}_{l_R}, \widehat{\boldsymbol{h}}_{l_R})$ and $(\boldsymbol{h}_{l_I}, \widehat{\boldsymbol{h}}_{l_I})$, including those that were repeated, one can deduce that EDAS-QSM contained many redundant calculations.

The premise behind RCEDAS-QSM was to remove these redundant calculations by eliminating the repetition of channel gain vector combinations. In doing so, all calculations in RCEDAS-QSM are unique. Consider the matrices shown above, which had previously been used

for EDAS-QSM. Once the repetitive channel gain vectors have been removed, the possible combinations of $(\boldsymbol{h}_{l_R}, \widehat{\boldsymbol{h}}_{l_R})$ and $(\boldsymbol{h}_{l_I}, \widehat{\boldsymbol{h}}_{l_I})$ can now be represented as:

$$(\boldsymbol{h}_{l_R}, \widehat{\boldsymbol{h}}_{l_R}) = \begin{pmatrix} (1,1) & (1,2) & (1,3) \\ 0 & (2,2) & (2,3) \\ 0 & 0 & (3,3) \end{pmatrix}$$

$$(\boldsymbol{h}_{l_I}, \widehat{\boldsymbol{h}}_{l_I}) = \begin{pmatrix} (1,1) & (1,2) & (1,3) \\ 0 & (2,2) & (2,3) \\ 0 & 0 & (3,3) \end{pmatrix}$$

By eliminating all repetitive calculations, RCEDAS-QSM remains optimal, but now has a lower computational complexity. The steps followed in order to reduce the computational complexity of EDAS-QSM is detailed below.

Step 1: Determine the total number of possible transmit antenna subsets.

$$N_S = \binom{N_{TOTAL}}{N_T} \tag{4.4}$$

Step 2: Determine all possible enumerations of channel gain vector pairs for each subset. The total number of possible enumerations for each subset is given by $\binom{N_T}{2}$, and each pair has the form $(\boldsymbol{h}_a, \boldsymbol{h}_b)$.

Step 3: Use the following matrices to determine all possible combinations of transmit antennas.

$$(\boldsymbol{h}_{l_R}, \widehat{\boldsymbol{h}}_{l_R}) = \begin{bmatrix} (\boldsymbol{h}_a, \boldsymbol{h}_a) & (\boldsymbol{h}_a, \boldsymbol{h}_b) \\ (0,0) & (\boldsymbol{h}_b, \boldsymbol{h}_b) \end{bmatrix} \tag{4.5}$$

$$(\boldsymbol{h}_{l_I}, \widehat{\boldsymbol{h}}_{l_I}) = \begin{bmatrix} (\boldsymbol{h}_a, \boldsymbol{h}_a) & (\boldsymbol{h}_a, \boldsymbol{h}_b) \\ (0,0) & (\boldsymbol{h}_b, \boldsymbol{h}_b) \end{bmatrix} \tag{4.6}$$

Step 4: Calculate the minimum ED between each vector pair, using the antenna combinations of (4.5) and (4.6).

$$ED_1^l = \min_{\substack{\boldsymbol{h}_{l_R} = \hat{\boldsymbol{h}}_{l_R} \\ \boldsymbol{h}_{l_I} = \hat{\boldsymbol{h}}_{l_I} \\ x_q, \hat{x}_q \in \tau \\ x_q \neq \hat{x}_q}} \left\| \boldsymbol{h}_{l_R} x_q^R + i\boldsymbol{h}_{l_I} x_q^I - \hat{\boldsymbol{h}}_{l_R} \hat{x}_q^R - i\hat{\boldsymbol{h}}_{l_I} \hat{x}_q^I \right\|_F^2 \tag{4.7}$$

$$ED_2^l = \min_{x_q, \hat{x}_q \in \tau} \left\| \boldsymbol{h}_{l_R} x_q^R + i\boldsymbol{h}_{l_I} x_q^I - \hat{\boldsymbol{h}}_{l_R} \hat{x}_q^R - i\hat{\boldsymbol{h}}_{l_I} \hat{x}_q^I \right\|_F^2 \tag{4.8}$$

$$ED^l = \min_{l \in [1:N_S]} \begin{bmatrix} ED_1^l & ED_2^l \end{bmatrix} \tag{4.9}$$

Step 5: Select the antenna pair that maximises the minimum ED.

$$l_{selected} = \underset{l \in [1:N_S]}{\operatorname{argmax}} \left(ED^l \right) \tag{4.10}$$

4.1.2.1 Analysis of Computational Complexity for RCEDAS-QSM

The computational complexity of RCEDAS-QSM is imposed by (4.7) and (4.8) in Step 4. Following Table 4.1, and similarly to EDAS-QSM, the complexity of the Frobenius norm operation in (4.7) is $(9N_R - 1)$. However, (4.7) is only valid in instances in which $\boldsymbol{h}_{l_R} = \hat{\boldsymbol{h}}_{l_R}$, $\boldsymbol{h}_{l_I} = \hat{\boldsymbol{h}}_{l_I}$ and $x_q \neq \hat{x}_q$. Based on (4.5) and (4.6), there are 4 instances in which $\boldsymbol{h}_{l_R} = \hat{\boldsymbol{h}}_{l_R}$ and $\boldsymbol{h}_{l_I} = \hat{\boldsymbol{h}}_{l_I}$. Furthermore, $x_q \neq \hat{x}_q$ occurs $(M^2 - M)$ times. Therefore, (4.7) is computed $4(M^2 - M)$ times, with the complexity of (4.7) being $4(M^2 - M)(9N_R - 1)$.

Once again, the complexity of the Frobenius norm operation in (4.8) is formulated as $(9N_R - 1)$. $\left\| \boldsymbol{h}_{l_R} x_q^R + i\boldsymbol{h}_{l_I} x_q^I - \hat{\boldsymbol{h}}_{l_R} \hat{x}_q^R - i\hat{\boldsymbol{h}}_{l_I} \hat{x}_q^I \right\|_F^2$ is calculated for all possible transmit symbols, and is therefore computed $5M^2$ times. The complexity of (4.8) is formulated as $5M^2(9N_R - 1)$. By adding the complexities of (4.7) and (4.8), the total number of flops required can be simplified as: $4M\big((9/4)M - 1\big)(9N_R - 1)$.

Lastly, similarly to EDAS-QSM, RCEDAS-QSM must be executed $\binom{N_T}{2} \times \binom{N_{TOTAL}}{N_T}$ times in total. Therefore, the computational complexity of RCEDAS-QSM is given as:

$$\delta_{RCEDAS-QSM} = 4M\left((9/4)M - 1\right)(9N_R - 1)\binom{N_T}{2}\binom{N_{TOTAL}}{N_T} \tag{4.11}$$

Full numerical comparisons of RCEDAS-QSM and EDAS-QSM are performed in Section 4.3.2. However, comparing the complexity of RCEDAS-QSM to EDAS-QSM, it can be seen that $4M\left((9/4)M - 1\right) < 4M(4M - 1)$. Based on the inequality, it can be concluded that RCEDAS-QSM has succeeded in reducing the complexity of EDAS-QSM.

4.2 Sub-Optimal Transmit Antenna Selection

EDAS is a selection criterion which yields optimal performance. However, its computational complexity is extremely high. Hence, this section serves as an investigation into the use of various sub-optimal, LCTAS schemes for QSM. The proposed schemes employs a combination of channel amplitude [39], antenna correlation [42, 44] and ED [32, 33] as the criterion used to select a subset of transmit antennas.

4.2.1 Capacity Optimised Antenna Selection for QSM

Rajashekar *et. al.* [39] first introduced capacity optimised antenna selection (COAS) as a novel transmit antenna selection scheme for SM. The principle behind COAS is that from the N_{TOTAL} transmit antennas, only N_T antennas are chosen. These N_T antennas correspond to those with the largest channel amplitudes. The results presented in [39] verified that COAS was capable of improving the error performance of SM, whilst imposing very low computational complexity. Motivated by this, COAS has been applied to QSM, and has been confirmed as the TAS algorithm which yields the lowest computational complexity.

Consider the $N_R \times N_{TOTAL}$ complex channel gain matrix $\boldsymbol{H}_T$, as depicted in Figure 4.1. The algorithm used to select the transmit antenna subset is as follows [39, 42]:

Step 1: Compute the norm of each element in the column vector $\boldsymbol{h}_j$

$$\left\|\boldsymbol{h}_j\right\|_F^2 \tag{4.12}$$

for $j \in [1 : N_{TOTAL}]$.

Step 2: Arrange the column vectors of $\boldsymbol{H}_T$ in descending order, such that:

$$\boldsymbol{H}_D = \left[\|\boldsymbol{h}_1\|_F^2 \geq \|\boldsymbol{h}_2\|_F^2 \geq \cdots \geq \left\|\boldsymbol{h}_{N_{TOTAL}}\right\|_F^2\right] \tag{4.13}$$

Step 3: Select the N_T largest channel gain vectors to form the $N_R \times N_T$ channel gain matrix $\boldsymbol{H}$.

4.2.1.1 Analysis of Computational Complexity for COAS-QSM

By applying a similar approach used in [42], it can be inferred that the computational complexity, or the number of flops, of COAS-QSM is imposed by Step 1. The Frobenius norm of each channel gain vector requires $2N_R - 1$ flops. This calculation is required for N_{TOTAL} vectors. As such, the total computational complexity is calculated as:

$$\delta_{COAS-QSM} = N_{TOTAL}(2N_R - 1) \tag{4.14}$$

4.2.2 Transmit Antenna Selection for QSM based on Amplitude and Antenna Correlation

TAS-A-C-QSM is based on the combination of two selection criterions, viz. channel amplitude [39] and antenna correlation [44]. The level of correlation between two transmit antennas can be ascertained by calculating the angle that is formed between the said antennas. This technique was first employed by Wang *et. al.* [18] in an SM detection algorithm known as SVD. In [18], the estimated antenna index was identified by selecting the channel gain vector which formed the smallest included angle with the received signal vector. Zhou *et. al.* [44] then stated that the existence of highly correlated transmit antennas causes an increase in detection errors. In other words, the smaller the correlation between transmit antennas, the better the overall system performance. By using [18] to calculate the angle between transmit antennas, [44] was able to eliminate the antennas with a high level of correlation.

Using the premise introduced in [44], transmit antenna selection based on amplitude and antenna correlation (TAS-A-C) was first proposed for SM by Pillay *et. al.* [42]. By applying the TAS-A-C algorithm to QSM, the authors of [43] were able to demonstrate that TAS-A-C-QSM improves the error performance of COAS-QSM. Therefore, TAS-A-C-QSM has proven to be capable of improving error performance, whilst maintaining a low-complexity approach to TAS.

The TAS-A-C-QSM scheme starts with an $N_R \times N_{TOTAL}$ channel gain matrix $\boldsymbol{H}_T$. As with all TAS, it is assumed that the channel information is perfectly known at the receiver. First, the $N_C = N_T + 1$ transmit antennas that correspond to the largest channel amplitudes are selected. Then, the correlation for all $\binom{N_C}{2}$ pairs of remaining antennas is evaluated by computing the angle between each channel gain vector pair [42, 44]. The transmit antenna pair that corresponds to the highest correlation, or smallest angle, is selected. Within the selected pair, the smaller channel vector is eliminated. This yields an $N_R \times N_T$ complex channel gain matrix $\boldsymbol{H}$. Following the approach taken in [42], the TAS-A-C-QSM algorithm may be formulated as follows [43]:

Step 1: Compute the channel amplitude of each column vector in $\boldsymbol{H}_T$

$$\bar{\boldsymbol{h}}_j = \left\|\boldsymbol{h}_j\right\|_F^2 \tag{4.15}$$

for $j \in [1 : N_{TOTAL}]$.

Step 2: Select the transmit antennas that correspond to the $N_C = N_T + 1$ largest channel amplitudes.

$$\boldsymbol{H}_{N_C} = [\bar{\boldsymbol{h}}_1 \;\; \bar{\boldsymbol{h}}_2 \;\; \cdots \;\; \bar{\boldsymbol{h}}_{N_C}] \tag{4.16}$$

where,

$$\bar{\boldsymbol{h}}_1 \geq \bar{\boldsymbol{h}}_2 \geq \cdots \geq \bar{\boldsymbol{h}}_{N_C}$$

Step 3: Determine all possible enumerations of channel gain vector pairs. The total number of possible vector pairs is given by $N_A = \binom{N_C}{2}$. Each pair will have the form $(\boldsymbol{h}_a, \boldsymbol{h}_b)$.

Step 4: Calculate the angle of correlation, θ, between both vectors of a vector pair [42, 44]. For each vector pair, θ can be calculated as:

$$\theta = \cos^{-1}\left(\frac{\left|\boldsymbol{h}_a{}^H \boldsymbol{h}_b\right|}{\|\boldsymbol{h}_a\|_F \, \|\boldsymbol{h}_b\|_F}\right) \tag{4.17}$$

The angle of correlation for each pair is stored in $\boldsymbol{A}_\theta$:

$$\boldsymbol{A}_\theta = [\theta_1 \quad \theta_2 \quad \cdots \quad \theta_{N_A}]$$

Step 5: Select the pair that results in the smallest angle θ (highest correlation), and eliminate the smaller of the two channel gain vectors. This forms the $N_R \times N_T$ complex channel gain matrix.

$$\boldsymbol{H} = [\boldsymbol{h}_1 \quad \boldsymbol{h}_2 \cdots \quad \boldsymbol{h}_{N_T}] \tag{4.18}$$

4.2.2.1 Analysis of Computational Complexity for TAS-A-C-QSM

From [42], it is shown that the computational complexity of TAS-A-C-QSM is imposed by Steps 1 and 4. Step 1 is based on COAS-QSM, where the computational complexity of calculating the Frobenius norm of N_{TOTAL} channel vectors is $N_{TOTAL}(2N_R - 1)$. Step 4 requires the angle of correlation to be calculated for $\binom{N_C}{2}$ transmit antenna pairs. For the numerator of (4.17), $2N_R$ flops are required. In order for the remainder of (4.17) to be computed, $4N_R + 2$ flops are required. Therefore, the number of flops required to calculate the angle of correlation is given by $(6N_R + 2)$. Hence, the total computational complexity imposed by TAS-A-C-QSM is given as [43]:

$$\delta_{TAS-A-C-QSM} = N_{TOTAL}(2N_R - 1) + (6N_R + 2)\binom{N_C}{2} \tag{4.19}$$

4.2.3 Low-Complexity Transmit Antenna Selection for QSM based on Amplitude and Antenna Correlation using the splitting technique

LCTAS-A-C-QSM is largely based on TAS-A-C-QSM and was introduced by Pillay *et. al.* [42]. LCTAS-A-C-QSM employs the same selection criterion as TAS-A-C-QSM, at a reduced complexity. The key idea behind LCTAS-A-C-QSM is to divide the $N_R \times N_{TOTAL}$ channel gain matrix $\boldsymbol{H}_T$, into two equal sub-matrices, before executing the remainder of the algorithm [42]. This is known as the splitting technique and is employed to significantly decrease the computational complexity of the algorithm.

For example, for a total of 10 transmit antennas, where only 4 antennas are required to be active for transmission, the total number of enumerations is given by $\binom{10}{4} = 210$. However, if the splitting technique is applied, we now have two sets of 5 antennas and must select 2 antennas from each set. Therefore, the number of enumerations for each set is given as $\binom{5}{2} = 10$, and the total number of enumerations for the scheme is only 20. Hence, it can be seen that utilising the splitting technique considerably reduces the computational complexity of an algorithm.

Similarly to TAS-A-C-QSM, the $N_L = \frac{1}{2}N_T + 1$ transmit antennas that correspond to the largest channel norms are chosen from each sub-matrix. The angle between each channel gain vector pair is then calculated. For each sub-matrix, the transmit antenna pair that has the highest correlation is selected, and the smaller channel vector within each pair is eliminated. The algorithm for the LCTAS-A-C-QSM scheme is as follows [42, 43]:

Step 1: Divide the $N_R \times N_{TOTAL}$ complex channel gain matrix $\boldsymbol{H}_T$ into two $N_R \times \frac{1}{2}N_{TOTAL}$ sub-matrices.

$$\boldsymbol{H}_1 = [\boldsymbol{h}_1 \;\; \boldsymbol{h}_2 \;\; \cdots \;\; \boldsymbol{h}_{N_1}] \tag{4.20}$$

$$\boldsymbol{H}_2 = [\boldsymbol{h}_{N_1+1} \;\; \boldsymbol{h}_{N_1+2} \;\; \cdots \;\; \boldsymbol{h}_{N_1+N_2}] \tag{4.21}$$

where $N_1 = N_2 = \frac{1}{2}N_{TOTAL}$.

Step 2: Compute the vector norm for sub-matrix $\boldsymbol{H}_1$ and $\boldsymbol{H}_2$, using (4.15).

Step 3: Select the antennas that correspond to the N_L largest channel amplitudes in each sub-matrix, i.e. $\boldsymbol{H}_1$ and $\boldsymbol{H}_2$.

$$\boldsymbol{H}_{N_{L1}} = [\boldsymbol{h}_1 \quad \boldsymbol{h}_2 \quad \cdots \quad \boldsymbol{h}_{N_L}] \tag{4.22}$$

$$\boldsymbol{H}_{N_{L_2}} = [\boldsymbol{h}_{N_1+1} \quad \boldsymbol{h}_{N_1+2} \quad \cdots \quad \boldsymbol{h}_{N_1+N_L}] \tag{4.23}$$

where $N_L = \frac{1}{2}N_T + 1$.

Step 4: Determine all possible enumerations of channel gain vector pairs for $\boldsymbol{H}_{N_{L1}}$ and $\boldsymbol{H}_{N_{L_2}}$. The total number of enumerations for each sub-matrix is given by $\binom{N_L}{2}$.

Step 5: Calculate the angle θ for each vector pair having the form $(\boldsymbol{h}_a, \boldsymbol{h}_b)$. The angle of correlation for all vector pairs in sub-matrices $\boldsymbol{H}_{N_{L1}}$ and $\boldsymbol{H}_{N_{L_2}}$ can be calculated by using (4.17).

Step 6: Select the pair that resulted in the smallest angle θ for sub-matrix $\boldsymbol{H}_{N_{L1}}$ and $\boldsymbol{H}_{N_{L_2}}$. Within each pair, eliminate the smaller channel gain vector. This forms two $N_R \times \frac{1}{2}N_T$ sub-matrices, $\boldsymbol{H}_{N_{T1}}$ and $\boldsymbol{H}_{N_{T2}}$.

Step 7: Combine sub-matrices $\boldsymbol{H}_{N_{T1}}$ and $\boldsymbol{H}_{N_{T2}}$ to form the $N_R \times N_T$ channel gain matrix $\boldsymbol{H}$.

$$\boldsymbol{H} = [\boldsymbol{H}_{N_{T1}} \quad \boldsymbol{H}_{N_{T2}}] \tag{4.24}$$

4.2.3.1 Analysis of Computational Complexity for LCTAS-A-C-QSM

The computational complexity associated with LCTAS-A-C-QSM is imposed by Steps 2 and 5 [42]. The computational complexity imposed by the operations in Steps 2 and 5 have been previously detailed TAS-A-C-QSM. In Step 2, the number of flops required to calculate the channel norms for N_{TOTAL} vectors is $N_{TOTAL}(2N_R - 1)$. In Step 5, the angle of correlation must be calculated for each sub-matrix, where each matrix has $\binom{N_L}{2}$ antenna pairs. The flops required

to calculate the angle θ for each sub-matrix is $(6N_R + 2)\binom{N_L}{2}$. Therefore, the total computational complexity of LCTAS-A-C-QSM is given by [42, 43]:

$$\delta_{LCTAS-A-C-QSM} = N_{TOTAL}(2N_R - 1) + 2(6N_R + 2)\binom{N_L}{2} \tag{4.25}$$

Comparing the complexity of LCTAS-A-C-QSM to TAS-A-C-QSM, it is observed that $2\binom{N_L}{2}$ will always be less than $\binom{N_C}{2}$. Therefore, it can be clearly established that LCTAS-A-C-QSM has indeed reduced the computational complexity of TAS-A-C-QSM.

4.2.4 Transmit Antenna Selection for QSM based on Amplitude, Antenna Correlation and Euclidean-Distance

A-C-ED-QSM is based on a LCTAS scheme first proposed in [42]. By employing a combination of three different TAS algorithms, viz. COAS-QSM, TAS-A-C-QSM and RCEDAS-QSM, A-C-ED-QSM is able to maximise the advantage of each algorithm, whilst minimising their disadvantages. In order to fully comprehend the advantages and disadvantages associated with each of the above-mentioned algorithms, the computational complexity of each TAS scheme is shown in Table 4.2. The complexity of a 2×2 4-QAM MIMO system with $N_{TOTAL} = 8$ is used as a numerical example in Table 4.2.

Table 4.2 Computational complexity of COAS-QSM, TAS-A-C-QSM and RCEDAS-QSM for $N_T \times N_R = 2 \times 2$, $N_{TOTAL} = 8$ and $M = 4$

TAS Schemes	Computational Complexity	No. of Flops
COAS-QSM	$\delta_{COAS-QSM} = N_{TOTAL}(2N_R - 1)$	24
TAS-A-C-QSM	$\delta_{TAS-A-C-QSM} = N_{TOTAL}(2N_R - 1) + (6N_R + 2)\binom{N_C}{2}$	66
RCEDAS-QSM	$\delta_{RCEDAS-QSM} = 4M\left((9/4)M - 1\right)(9N_R - 1)\binom{N_T}{2}\binom{N_{TOTAL}}{N_T}$	60,928

Based on the complexities shown in Table 4.2, one can clearly observe that COAS-QSM imposes the lowest computational complexity, followed closely by TAS-A-C-QSM. In order for A-C-ED-QSM to be a viable LCTAS scheme, COAS-QSM and TAS-A-C-QSM should be implemented when a large number of calculations are required. Although RCEDAS-QSM imposes a large computational complexity, it is an optimal TAS scheme. Hence, in order to reap the benefits of optimal TAS, RCEDAS-QSM should be incorporated at a stage in which minimal calculations are required.

As with any TAS algorithm, A-C-ED-QSM starts by analysing all N_{TOTAL} transmit antennas. Since the first step requires the largest number of calculations, and COAS-QSM has the lowest complexity, it is the first algorithm to be executed. Based on COAS, A-C-ED-QSM first selects the antennas that correspond to the $N_E = N_T + 2$ largest channel gain vectors.

At this stage, only N_E transmit antennas remain, with TAS-A-C-QSM having the lowest complexity between the remaining unused algorithms. Therefore, TAS-A-C-QSM is executed next. The correlation between the N_E antennas are calculated by computing the angle between the $\binom{N_E}{2}$ channel gain vector pairs. The vector pair resulting in the highest correlation is selected, and the smaller channel gain vector is eliminated.

In the final step, $N_F = N_T + 1$ antennas remain. Due to the high complexity of RCEDAS-QSM, it is the last algorithm to be performed. For the remaining N_F antennas, there exists $\binom{N_F}{N_T}$ antenna subsets. For each subset, the minimum ED between transmit vectors is determined. The antenna subset which maximises the minimum ED is selected for transmission.

The proposed A-C-ED-QSM algorithm is detailed as follows:

Step 1: Compute the vector norm of each column vector in $\boldsymbol{H}_T$.

$$\left\|\boldsymbol{h}_j\right\|_F^2 \tag{4.26}$$

for $j \in [1 : N_{TOTAL}]$.

Step 2: Select the transmit antennas that correspond to the N_E largest channel amplitudes.

$$\boldsymbol{H}_{N_E} = [\boldsymbol{h}_1 \quad \boldsymbol{h}_2 \quad \cdots \quad \boldsymbol{h}_{N_E}] \tag{4.27}$$

where $N_E = N_T + 2$.

Step 3: Determine all possible channel gain vector pairs, where the total number of vector pairs is given by $\binom{N_E}{2}$. Each vector pair has the form $(\boldsymbol{h}_a, \boldsymbol{h}_b)$.

Step 4: Calculate the angle between the vectors of each vector pair.

$$\theta = \cos^{-1}\left(\frac{\left|\boldsymbol{h}_a{}^H \boldsymbol{h}_b\right|}{\|\boldsymbol{h}_a\|_F \, \|\boldsymbol{h}_b\|_F}\right)$$

Step 5: Select the vector pair which yields the smallest angle θ. Within this pair, eliminate the channel gain vector with the smaller amplitude. This results in an $N_F \times N_R$ channel gain matrix, where $N_F = N_T + 1$.

Step 6: The total number of transmit antenna subsets is $\binom{N_F}{N_T}$. For each subset, determine all possible enumerations of vector pairs. The total number of possible enumerations for each set is given by $\binom{N_T}{2}$.

Step 7: Based on the RCEDAS-QSM algorithm, calculate the minimum ED of each vector pair, using (4.7) and (4.8).

Step 8: Determine the minimum ED for each antenna subset.

Step 9: Select the antenna subset that maximises the minimum ED between all transmit vectors.

4.2.4.1 Analysis of Computational Complexity for A-C-ED-QSM

Since A-C-ED-QSM is based on a combination of COAS-QSM, TAS-A-C-QSM and RCEDAS-QSM, the computational complexity of A-C-ED-QSM can be easily determined by using the complexity of each TAS algorithm. The complexity imposed by each algorithm has been thoroughly detailed in Sections 4.1.2, 4.2.1 and 4.2.2.

The computational complexity of A-C-ED-QSM is imposed by Steps 1, 4 and 7. Step 1 computes the vector norm for N_{TOTAL} elements, requiring $N_{TOTAL}(2N_R - 1)$ flops. Step 4 calculates the angle of correlation between $\binom{N_E}{2}$ vector pairs. Similarly to TAS-A-C-QSM, the angle of correlation for all pairs requires $(6N_R + 2)\binom{N_E}{2}$ flops for execution. Lastly, Step 7 calculates the ED of $\binom{N_F}{N_T}$ antenna subsets. Therefore, based on the complexity of RCEDAS-QSM, the complexity of Step 7 is given as: $4M\big((9/4)M - 1\big)(9N_R - 1)\binom{N_T}{2}\binom{N_F}{N_T}$. Thus, the overall computational complexity imposed by executing A-C-ED is:

$$\delta_{A-C-ED-QSM} = N_{TOTAL}(2N_R - 1) + (6N_R + 2)\binom{N_E}{2} + 4M\big((9/4)M - 1\big)(9N_R - 1)\binom{N_T}{2}\binom{N_F}{N_T} \tag{4.28}$$

4.3 Simulation Results and Discussion

In this section, Monte Carlo simulation results are presented for the QSM scheme. Monte Carlo simulation results for conventional SM have also been presented to serve as a basis of comparison for the performance of QSM. In addition, Monte Carlo simulation results for the proposed EDAS-QSM, RCEDAS-QSM, COAS-QSM, TAS-A-C-QSM, LCTAS-A-C-QSM and A-C-ED-QSM schemes have been produced in Rayleigh flat fading channels.

The performance of the various TAS algorithms have been separated in terms of the BER performance and the computational complexity associated with each scheme. These results are presented and analysed in detail below.

4.3.1 Bit Error Performance

The average BER versus the average SNR per symbol was evaluated for various spectral efficiencies, i.e. 4, 6 and 8 b/s/Hz. For each spectral efficiency, the error performance of SM [9, 12-14], QSM [30, 31] and the proposed schemes, viz. EDAS-QSM, RCEDAS-QSM, COAS-QSM [43], TAS-A-C-QSM [43], LCTAS-A-C-QSM [43] and A-C-ED-QSM have been evaluated.

As mentioned previously, when TAS is applied to QSM, N_{TOTAL} transmit antennas are required. From these N_{TOTAL} antennas, only N_T antennas are selected and utilised for

transmission, where $N_T < N_{TOTAL}$. It must be noted that due to the nature of the LCTAS-A-C-QSM algorithm, N_{TOTAL} must be divisible by 2.

For all Monte Carlo simulations, it is assumed that the channel information is perfectly known at the receiver. Furthermore, optimal ML detection has been employed in all cases. For the aforementioned schemes, x_q denotes the q^{th} symbol from a square M-QAM constellation, with $E[|x_q|^2] = 1$ and $q \in [1: M]$.

The notation used to denote the configuration of SM and QSM is (M, N_T, N_R) and the notation used to denote EDAS-QSM, RCEDAS-QSM and COAS-QSM is (M, N_{TOTAL}, N_T, N_R). The configuration of TAS-A-C-QSM and LCTAS-A-C-QSM is represented as (M, N_{TOTAL}, N, N_R), where $N = N_C$ and $N = N_L$, respectively. Lastly the notation used to denote A-C-ED-QSM is $(M, N_{TOTAL}, N_T, N_E, N_F, N_R)$.

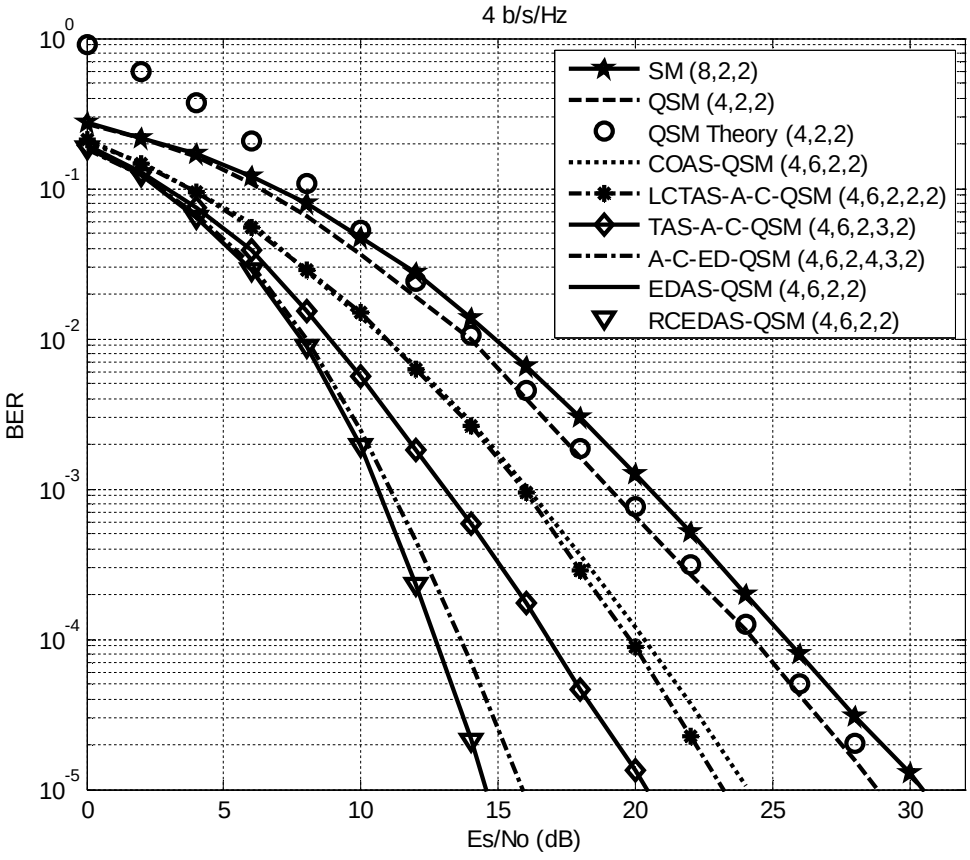

Figure 4.2 BER performance of TAS for QSM for 4 b/s/Hz and $N_R = 2$

Figure 4.2 illustrates the BER performance of the aforementioned TAS algorithms for QSM, when $N_R = 2$. For the purposes of fair comparison, all TAS algorithms have been compared when $N_{TOTAL} = 6$. At a BER of 10^{-5}, COAS-QSM and LCTAS-A-C-QSM surpasses the error performance of QSM, with an approximate SNR gain of 4.71 dB and 5.56 dB, respectively. EDAS-QSM and RCEDAS-QSM match closely, with an SNR gain of 14.41 dB. It is also noted that A-C-ED-QSM outperforms TAS-A-C-QSM. Compared to QSM, A-C-ED-QSM displays a 12.64 dB SNR gain, whilst TAS-A-C-QSM exhibits an SNR gain of 8.24 dB.

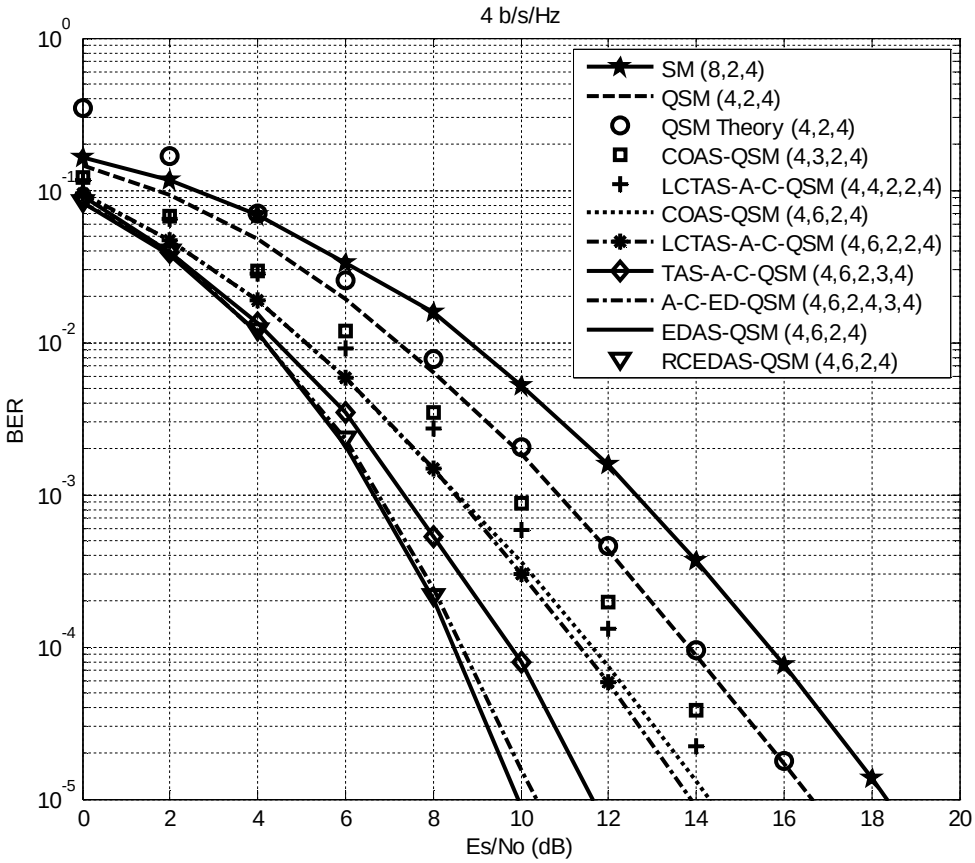

Figure 4.3 BER performance of TAS for QSM for 4 b/s/Hz and $N_R = 4$

Study of the various TAS performance graphs has shown a clear improvement in the error performance of QSM. For example (refer to Figure 4.3), at a BER of 10^{-5}, COAS-QSM has a 1.18 dB gain over QSM, when $N_{TOTAL} = 3$. However, this gain can be further improved by increasing N_{TOTAL}. For instance, when N_{TOTAL} is increased to 6, COAS-QSM exhibits a 2.36 dB gain over QSM. When $N_{TOTAL} = 4$, LCTAS-A-C-QSM has a 1.81 dB SNR gain over QSM. However, when $N_{TOTAL} = 6$, the SNR gain of LCTAS-A-C-QSM compared to QSM increases to

2.91 dB. Therefore, the concept of improving error performance by increasing the total number of transmit antennas is corroborated by the two TAS schemes.

Furthermore, for a BER of 10^{-5}, LCTAS-A-C-QSM outperforms COAS-QSM by 0.55 dB. LCTAS-A-C-QSM was further outperformed by TAS-A-C-QSM and A-C-ED-QSM. TAS-A-C-QSM and A-C-ED-QSM exhibit a 4.91 dB and 6.18 dB SNR gain over QSM, respectively. RCEDAS-QSM and EDAS-QSM match closely, with an approximate SNR gain of 6.75 dB as compared to QSM.

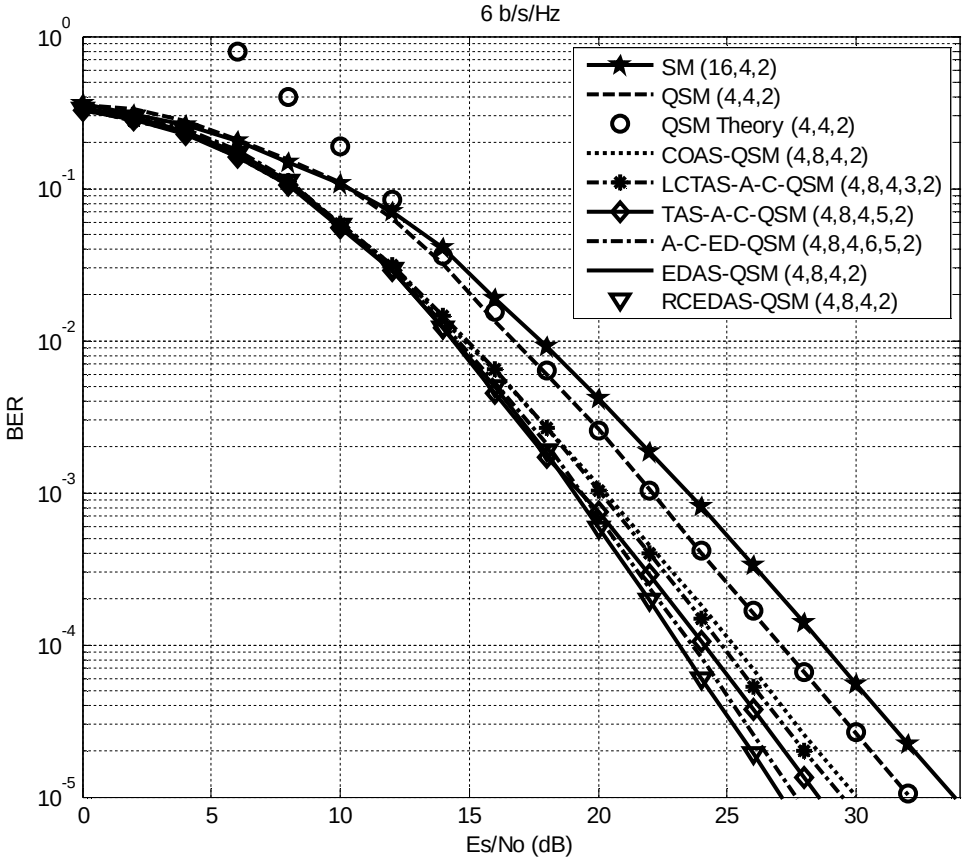

Figure 4.4 BER performance of TAS for QSM for 6 b/s/Hz and $N_R = 2$

Figure 4.4 depicts the behaviour of the aforementioned TAS schemes for a spectral efficiency of 6 b/s/Hz and $N_R = 2$. COAS-QSM, LCTAS-A-C-QSM, TAS-A-C-QSM, A-C-ED-QSM have SNR gains of 2.18 dB, 2.69 dB, 3.86 dB and 4.50 dB over QSM, respectively. EDAS-QSM and RCEDAS-QSM match closely with an SNR gain of approximately 5.25 dB.

In Figure 4.5, optimal and sub-optimal TAS algorithms have been applied to a QSM configuration, with a spectral efficiency of 6 b/s/Hz. All Monte Carlo simulations illustrated in Figure 4.5 have used $N_R = 4$.

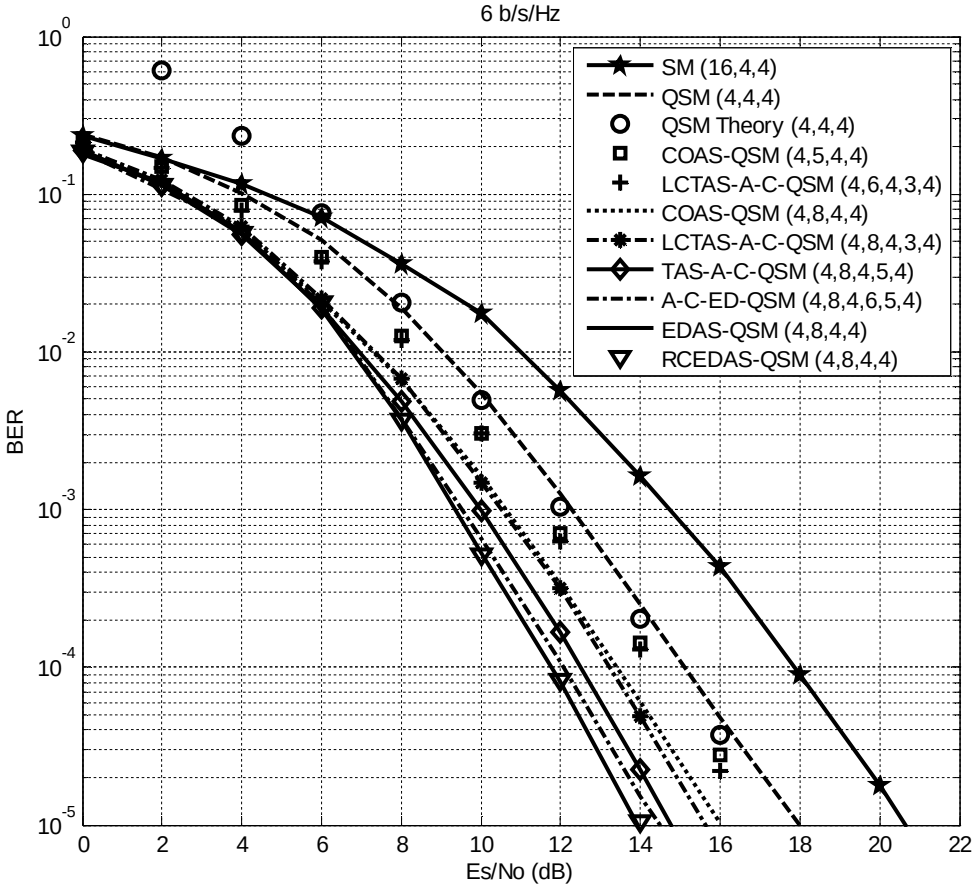

Figure 4.5 BER performance of TAS for QSM for 6 b/s/Hz and $N_R = 4$

At a BER of 10^{-5} and $N_{TOTAL} = 5$, COAS-QSM has an SNR gain of 0.90 dB over QSM. However, this increases to a gain of 2.10 dB when N_{TOTAL} is increased to 8. Similarly, for $N_{TOTAL} = 6$, LCTAS-A-C-QSM has an approximate SNR gain of 1.15 dB compare to QSM. However, increasing N_{TOTAL} to 8 results in a 2.50 dB gain over QSM. It is once again noted that by increasing the value of N_{TOTAL}, one can increase the overall BER performance of a TAS scheme.

Comparing the TAS schemes of Figure 4.5 for $N_{TOTAL} = 8$, COAS-QSM, LCTAS-A-C-QSM, TAS-A-C-QSM and A-C-ED-QSM improve upon QSM by 2.10 dB, 2.50 dB, 3.16 dB and 3.50 dB, respectively. Lastly, EDAS-QSM and RCEDAS-QSM both have an estimated SNR gain of 3.90 dB over QSM.

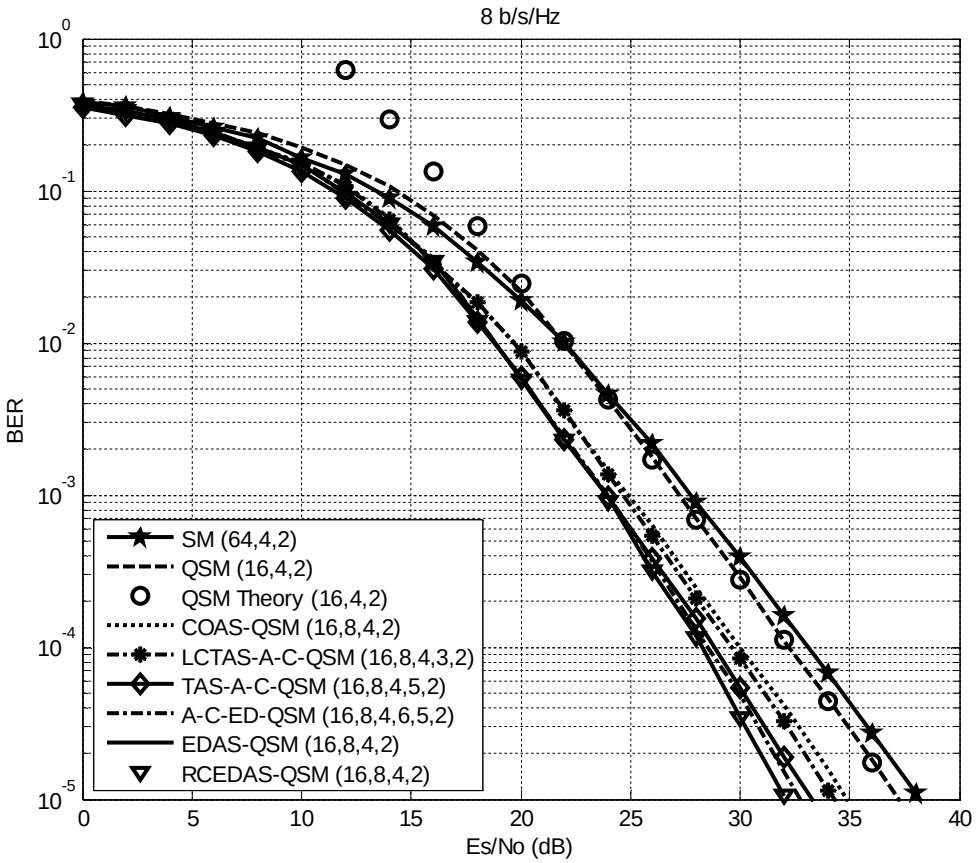

Figure 4.6 BER performance of TAS for QSM for 8 b/s/Hz and $N_R = 2$

From Figure 4.6, it is evident that the error performance of EDAS-QSM and RCEDAS-QSM closely match each other, whilst significantly improving the error performance of QSM. EDAS-QSM and by consequence, RCEDAS-QSM, has an SNR gain of 5.13 dB over QSM. Similarly to the results presented previously, COAS-QSM has an SNR gain of 2.06 dB over QSM, followed by LCTAS-A-C-QSM, TAS-A-C-QSM and A-C-ED-QSM, each with an SNR gain of 2.55 dB, 3.45 dB and 4.23 dB, in that order.

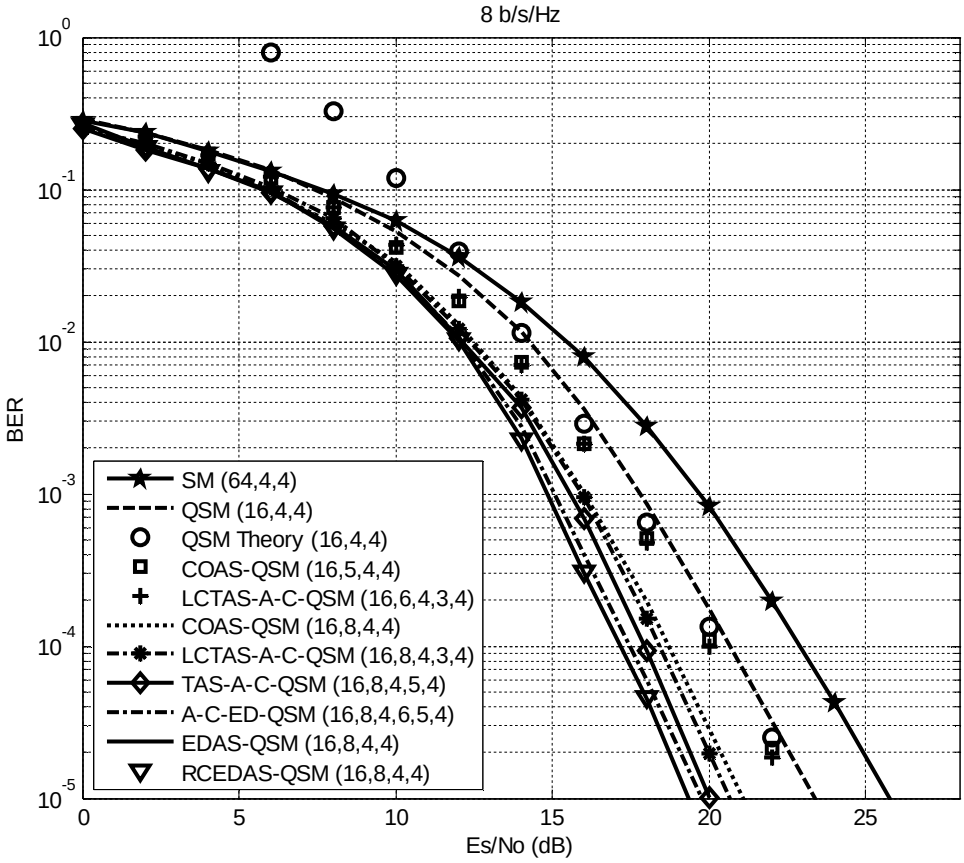

Figure 4.7 BER performance of TAS for QSM for 8 b/s/Hz and $N_R = 4$

Lastly, Figure 4.7 considers the BER performance of TAS for QSM, with a spectral efficiency of 8 b/s/Hz and $N_R = 4$. Even whilst spectral efficiency is increased, it is noted that increasing N_{TOTAL} continues to improve the error performance of TAS algorithms. By increasing the value of N_{TOTAL}, the SNR gain of COAS-QSM and LCTAS-A-C-QSM has notably improved. Compared to the BER performance of QSM at 10^{-5} and when $N_{TOTAL} = 8$, COAS-QSM, LCTAS-A-C-QSM, TAS-A-C-QSM, A-C-ED-QSM, EDAS-QSM and RCEDAS-QSM, each have an estimated SNR gain of 1.98 dB, 2.35 dB, 2.96 dB, 3.23 dB and 3.73 dB, respectively.

At a BER of 10^{-5}, the SNR gains achieved by each TAS algorithm, with respect to QSM, has been tabulated in Table 4.3 and Table 4.4. The SNR gains have been categorised for systems where $N_R = 2$ and $N_R = 4$. Furthermore, the configurations employed by QSM have also been indicated.

Table 4.3 Comparison of the SNR gain of proposed TAS algorithms with respect to QSM, for $N_R = 2$

Configuration	SNR Gain (dB)					
	EDAS-QSM	**RCEDAS-QSM**	**COAS-QSM**	**TAS-A-C-QSM**	**LCTAS-A-C-QSM**	**A-C-ED-QSM**
$M = 4$, $N_{TOTAL} = 6$, $N_T = 2$	14.41	14.41	4.71	8.24	5.56	12.64
$M = 4$, $N_{TOTAL} = 8$, $N_T = 4$	5.25	5.25	2.18	3.86	2.69	4.50
$M = 16$, $N_{TOTAL} = 8$, $N_T = 4$	5.13	5.13	2.06	3.45	2.55	4.23

Table 4.4 Comparison of the SNR gain of proposed TAS algorithms with respect to QSM, for $N_R = 4$

Configuration	SNR Gain (dB)					
	EDAS-QSM	**RCEDAS-QSM**	**COAS-QSM**	**TAS-A-C-QSM**	**LCTAS-A-C-QSM**	**A-C-ED-QSM**
$M = 4$, $N_{TOTAL} = 6$, $N_T = 2$	6.75	6.75	2.36	4.91	2.91	6.18
$M = 4$, $N_{TOTAL} = 8$, $N_T = 4$	3.90	3.90	2.10	3.16	2.50	3.50
$M = 16$, $N_{TOTAL} = 8$, $N_T = 4$	3.73	3.73	1.98	2.96	2.35	3.23

EDAS-QSM and RCEDAS-QSM provide the largest SNR gains over QSM due to the use of ED as a selection criterion. A-C-ED-QSM incorporates ED as a selection criterion, thereby providing it with the largest SNR gain compared to the alternate sub-optimal algorithms. This is followed by TAS-A-C-QSM and LCTAS-A-C-QSM, which includes the use of both channel amplitude and antenna correlation as selection criteria. Lastly, COAS-QSM exhibits a minimal SNR gain due to the use of channel amplitude as the only selection criterion.

4.3.2 Complexity Analysis

At this stage, it has clearly been shown that QSM is an innovative way of improving upon the spectral efficiency and error performance of conventional SM. However, the error performance of QSM can be further enhanced by implementing TAS techniques, such as EDAS-QSM, RCEDAS-QSM, COAS-QSM, TAS-A-C-QSM, LCTAS-A-C-QSM and A-C-ED-QSM. A summary of the computational complexity imposed by each algorithm is shown in Table 4.5.

Table 4.5 Summary of computational complexity imposed by each TAS algorithm

Transmit Antenna Selection Schemes	Computational Complexity
EDAS-QSM	$\delta_{EDAS-QSM} = 4M(4M-1)(9N_R-1)\binom{N_T}{2}\binom{N_{TOTAL}}{N_T}$
RCEDAS-QSM	$\delta_{RCEDAS-QSM} = 4M\big((9/4)M-1\big)(9N_R-1)\binom{N_T}{2}\binom{N_{TOTAL}}{N_T}$
COAS-QSM	$\delta_{COAS-QSM} = N_{TOTAL}(2N_R-1)$
TAS-A-C-QSM	$\delta_{TAS-A-C-QSM} = N_{TOTAL}(2N_R-1) + (6N_R+2)\binom{N_C}{2}$
LCTAS-A-C-QSM	$\delta_{LCTAS-A-C-QSM} = N_{TOTAL}(2N_R-1) + 2(6N_R+2)\binom{N_L}{2}$
A-C-ED-QSM	$\delta_{A-C-ED-QSM} = N_{TOTAL}(2N_R-1) + (6N_R+2)\binom{N_E}{2} + 4M\big((9/4)M-1\big)(9N_R-1)\binom{N_T}{2}\binom{N_F}{N_T}$

A numerical comparison of the computational complexity imposed by the aforementioned TAS algorithms is tabulated for the configurations employed in Figure 4.3 - Figure 4.7. This comparison is tabulated in Table 4.6. The notation used to denote the configuration of each TAS algorithm is: (M, N_{TOTAL}, N_T, N_R).

Table 4.6 Numerical comparison of computational complexity imposed by various TAS algorithms

Configuration	Complexity					
	EDAS-QSM	**RCEDAS-QSM**	**COAS-QSM**	**TAS-A-C-QSM**	**LCTAS-A-C-QSM**	**A-C-ED-QSM**
$(4, 6, 2, 2)$ $N_L = 2, N_C = 3,$ $N_E = 4, N_F = 3$	61,200	32,640	18	60	46	6,630
$(4, 6, 2, 4)$ $N_L = 2, N_C = 3,$ $N_E = 4, N_F = 3$	126,000	67,200	42	120	94	13,638
$(4, 8, 4, 2)$ $N_L = 3, N_C = 5,$ $N_E = 6, N_F = 5$	1,713,600	913,920	24	164	108	65,514
$(4, 8, 4, 4)$ $N_L = 3, N_C = 5,$ $N_E = 6, N_F = 5$	3,528,000	1,881,600	56	316	212	269,246
$(16, 8, 4, 2)$ $N_L = 3, N_C = 5,$ $N_E = 6, N_F = 5$	28,788,480	15,993,600	24	164	108	1,142,634
$(16, 8, 4, 4)$ $N_L = 3, N_C = 5,$ $N_E = 6, N_F = 5$	59,270,400	32,928,000	56	316	212	4,704,446

Consider the configuration of $M = 4, N_{TOTAL} = 8, N_T = 4$ and $N_R = 4$. The computational complexity imposed by EDAS-QSM is undoubtedly high. However, by employing RCEDAS-QSM, the complexity of EDAS-QSM is reduced by 46.67 %. In addition, four LCTAS algorithms have been applied to QSM, viz. A-C-ED-QSM, TAS-A-C-QSM, LCTAS-A-C-QSM and COAS-QSM. Of these four algorithms, the SNR gains summarised in Table 4.4 show that A-C-ED-QSM demonstrates the most significant improvement in error performance. Although the performance of A-C-ED-QSM surpasses that of other LCTAS schemes, it has the highest computational complexity. However, when compared to RCEDAS-QSM, A-C-ED-QSM exhibited a 79.71 % reduction in the computational complexity.

Figure 4.8 and Figure 4.9 illustrates a graphical representation of the computational complexity imposed by each TAS algorithm. Using the equations summarised in Table 4.5, and a configuration of $N_{TOTAL} = 8$, $N_T = 4$ and $N_R = 4$, the complexity of the aforementioned TAS algorithms for various M-QAM modulation orders has been depicted, i.e. the complexity of each algorithm when $M = 4$, $M = 16$ and $M = 64$ has been documented.

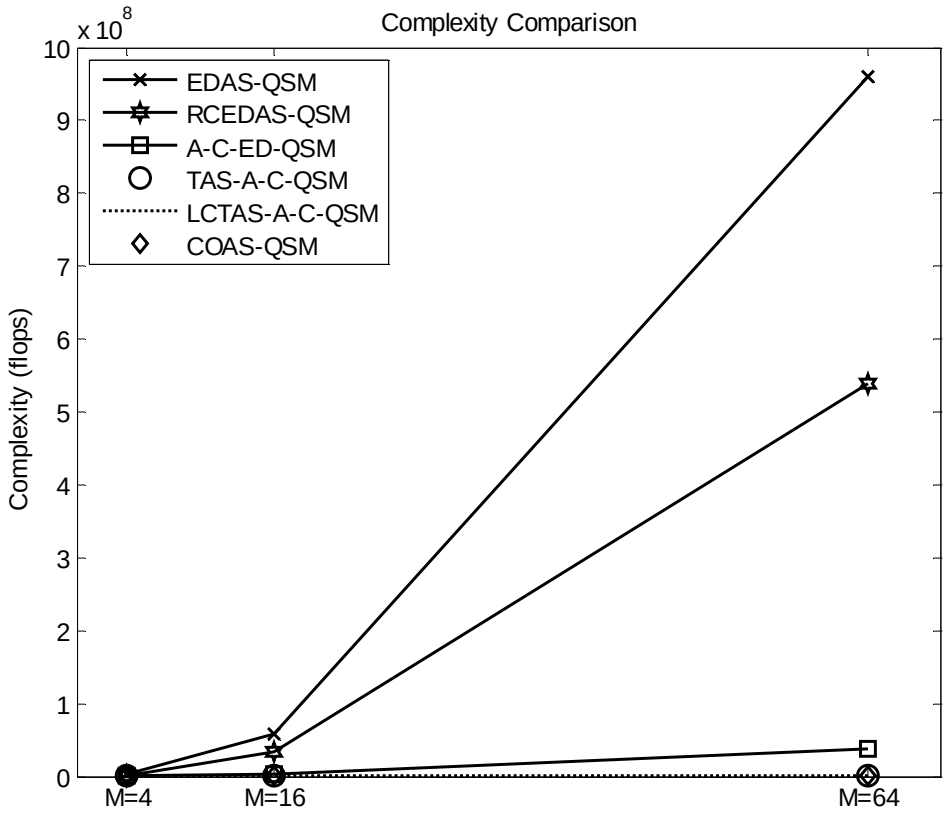

Figure 4.8 Computational complexity comparison of TAS algorithms for $M = 4$, $M = 16$ and $M = 64$

Based on the results depicted in Figure 4.8, it is noted that the complexity imposed by LCTAS-A-C-QSM, COAS-QSM and TAS-A-C-QSM is substantially lower than EDAS-QSM and RCEDAS-QSM. As expected, EDAS-QSM imposes the highest computational complexity, followed by RCEDAS-QSM. RCEDAS-QSM and A-C-ED-QSM achieves a considerable reduction in complexity, with respect to EDAS-QSM. It is also noted that the complexity of EDAS-QSM, RCEDAS-QSM and A-C-ED-QSM is dependent on the modulation order, M. In other words, as M increases, so too does the computational complexity of EDAS-QSM, RCEDAS-QSM and A-C-ED-QSM.

Figure 4.9 illustrates the computational complexity of COAS-QSM, TAS-A-C-QSM and LCTAS-A-C-QSM. Upon closer inspection, it is clear that the TAS algorithms depicted in Figure 4.9 are independent of the modulation order, M. This means that COAS-QSM, TAS-A-C-QSM and LCTAS-A-C-QSM relies exclusively on the values of N_{TOTAL}, N_R and N_T.

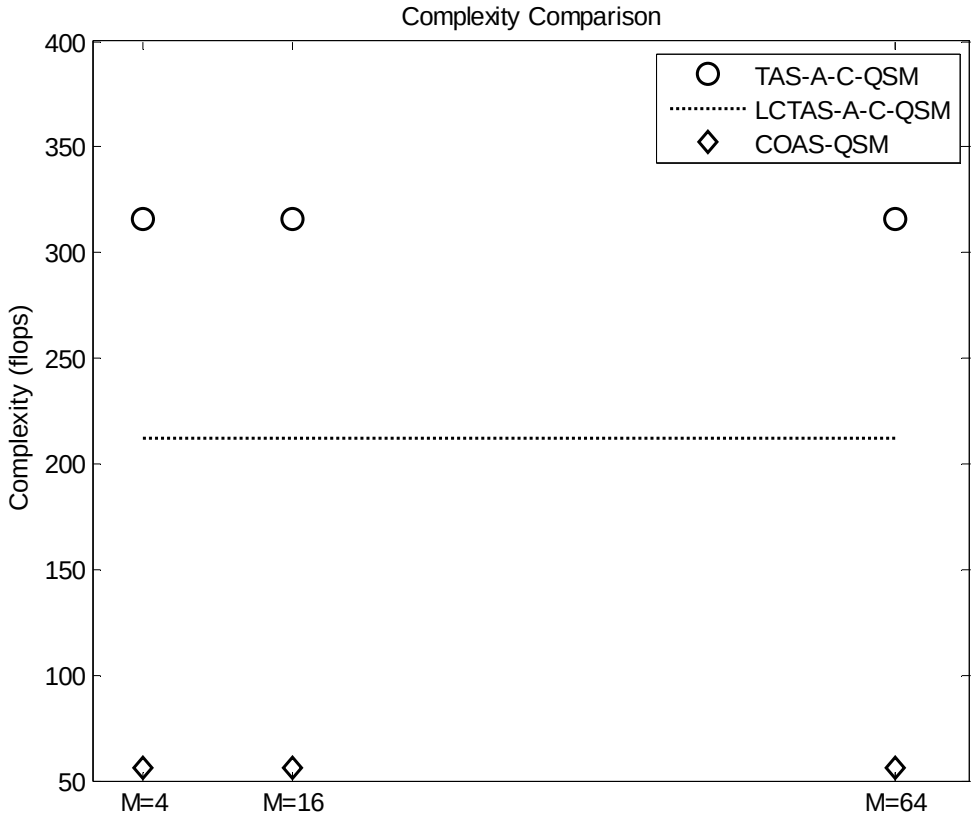

Figure 4.9 Computational complexity comparison of TAS-A-C-QSM, LCTAS-A-C-QSM and COAS-QSM for $M = 4$, $M = 16$ and $M = 64$

When compared to the four LCTAS techniques, RCEDAS-QSM still has a significantly higher computational complexity. Although RCEDAS-QSM has a higher computational complexity, it remains an optimal TAS technique, and therefore results in significant improvements in error performance. COAS-QSM has the lowest computational complexity compared to the alternate TAS schemes. However, COAS-QSM also displays the smallest improvement in BER performance. Hence, there evidently exists a trade-off between improving error performance and increasing computational complexity.

This chapter has confirmed that the concept of applying TAS to QSM is advantageous, especially in terms of reducing the error performance of QSM. Within this chapter, several optimal and sub-optimal TAS algorithms have been applied to QSM, and their BER performance has been documented accordingly. The results presented Section 4.3 has shown that each TAS algorithm is beneficial, either in terms of reducing error performance, or minimising computational complexity.

5 CONCLUSION

5.1 Discussion

The purpose of this dissertation was to first investigate the use of QSM as an innovative way of overcoming the limitations suffered by SM. One such drawback is that the spectral efficiency of SM is only able to increase in proportion to the base two logarithm of the number of transmit antennas. QSM had previously been proposed as an inventive solution to overcome the restricted spectral efficiency of SM.

The starting point of this dissertation was to verify that QSM both increased the spectral efficiency, as well as improved the error performance, of SM. Table 5.1 summarises the performance gains achieved by QSM as compared to SM.

Table 5.1 Comparison of the SNR gain (dB) of QSM as compared to SM at a BER of 10^{-5}

Configuration	$M = 4, N_T = 2$	$M = 4, N_T = 4$	$M = 16, N_T = 4$
$N_R = 2$	1.67	1.47	1.17
$N_R = 4$	1.94	2.94	2.33

Literature has demonstrated that the error performance of open-loop MIMO systems can be further improved by applying TAS. This served as the first contribution of this dissertation. This concept was verified by applying several TAS algorithms to QSM. EDAS-QSM was implemented as an optimal TAS algorithm. As expected, EDAS-QSM resulted in a substantial improvement in the error performance of QSM.

It is a well-documented fact that optimal antenna selection techniques suffer from severely high computational complexity. Therefore, it was imperative to reduce the complexity imposed by EDAS-QSM, whilst simultaneously maintaining its superior error performance. On this note, RCEDAS-QSM was proposed as an optimal TAS algorithm which reduced the complexity of EDAS-QSM. Monte Carlo simulations verified that RCEDAS-QSM closely matched the BER performance of EDAS-QSM, whilst simultaneously reducing the complexity of EDAS-QSM.

As previously mentioned, a notable disadvantage of optimal antenna selection is the extremely high computational complexity it imposes. In order to mitigate the disadvantage experienced by optimal TAS, this dissertation further proposed the implementation of four sub-optimal LCTAS algorithms, viz. COAS-QSM, TAS-A-C-QSM, LCTAS-A-C-QSM and A-C-ED-QSM. LCTAS proved to be beneficial in the sense that the error performance of QSM was improved upon, without drastically increasing computational complexity. The SNR gain achieved by each TAS algorithms, with respect to QSM, is tabulated in Table 5.2. The configuration of each TAS algorithm is denoted by (M, N_{TOTAL}, N_T, N_R).

Table 5.2 Summary of the SNR gains of each TAS algorithm, as compared to QSM, at a BER of 10^{-5}

Configuration	SNR Gain (dB)					
	EDAS-QSM	**RCEDAS-QSM**	**COAS-QSM**	**TAS-A-C-QSM**	**LCTAS-A-C-QSM**	**A-C-ED-QSM**
(4,6,2,2)	14.41	14.41	4.71	8.24	5.56	12.64
(4,6,2,4)	6.75	6.75	2.36	4.91	2.91	6.18
(4,8,4,2)	5.25	5.25	2.18	3.86	2.69	4.50
(4,8,4,4)	3.90	3.90	2.10	3.16	2.50	3.50
(16,8,4,2)	5.13	5.13	2.06	3.45	2.55	4.23
(16,8,4,4)	3.73	3.73	1.98	2.96	2.35	3.23

The second contribution of this dissertation was to evaluate the computational complexity of each TAS algorithm. As expected, the computational complexity imposed by EDAS-QSM was found to be excessively high. Employing RCEDAS-QSM reduced the complexity of EDAS-QSM by 46.67 %, whilst maintaining optimal error performance. Additionally, the computational complexity of each of the four LCTAS algorithms were formulated. The computational complexity of each TAS algorithm is compared in Table 5.3. Once again, the configuration of each TAS algorithm is denoted by (M, N_{TOTAL}, N_T, N_R).

Table 5.3 Comparison of computational complexity of TAS algorithms

Configuration	Complexity					
	EDAS-QSM	**RCEDAS-QSM**	**COAS-QSM**	**TAS-A-C-QSM**	**LCTAS-A-C-QSM**	**A-C-ED-QSM**
$(4, 6, 2, 2)$	61,200	32,640	18	60	46	6,630
$(4, 6, 2, 4)$	126,000	67,200	42	120	94	13,638
$(4, 8, 4, 2)$	1,713,600	913,920	24	164	108	65,514
$(4, 8, 4, 4)$	3,528,000	1,881,600	56	316	212	269,246
$(16, 8, 4, 2)$	28,788,480	15,993,600	24	164	108	1,142,634
$(16, 8, 4, 4)$	59,270,400	32,928,000	56	316	212	4,704,446

Based on the SNR gains presented in Table 5.2, A-C-ED-QSM was established as the best performing sub-optimal algorithm. Furthermore, A-C-ED-QSM was found to have reduced the complexity of RCEDAS-QSM by 79.71 %. However, Table 5.3 shows that, of the sub-optimal algorithms, A-C-ED-QSM also imposes the highest complexity. In addition, it was observed that when compared to the other TAS algorithms, COAS-QSM exhibited the lowest computational complexity. However, it is also noted that COAS-QSM exhibited the poorest error performance amongst the TAS algorithms. Similarly, although TAS-A-C-QSM and LCTAS-A-C-QSM impose low computational complexities, the end result of employing these algorithms is that there is a minimal improvement in BER performance. Consequently, a trade-off between increasing computational complexity and improving BER performance is evident.

Each TAS algorithm that has been presented has its own advantages, such as low complexity or optimal error performance. The selection and implementation of one of these algorithms would therefore depend solely on the requirements of the real-world scenario.

5.2 Future Work

QSM is a novel, SM-based MIMO scheme, which capitalises on the advantages of SM, whilst further improving upon its spectral efficiency. The introduction of QSM is a fairly recent one, and as a result, it has yet to be extensively researched in literature. If meticulously explored, there are many avenues of QSM that could prove to be beneficial. One such avenue is the use of alternate closed-loop designs for QSM. Moreover, combining QSM with OFDM in order to improve the spectral efficiency and error performance of QSM is a topic which must be further explored. Another area of interest, which requires further investigation, is the use of alternate detection algorithms for QSM. ML-based detection is the only form of detection considered for QSM. As previously mentioned, this detection algorithm is optimal, and as a result, the computational complexity it imposes is considerably high. Therefore, it would be advantageous to explore the use of alternate detection schemes, which would be capable of providing near-optimal error performance at a fraction of the computational complexity.

REFERENCES

[1] K. Liu, Cooperative communications and networking, Cambridge: Cambridge University Press, 2009.

[2] J. H. Winters, "On the Capacity of Radio Communication Systems with Diversity in a Rayleigh Fading Environment," in *IEEE Journal on Selected Areas in Communications*, vol. 5, no. 5, pp. 871-878, Jun. 1987.

[3] G. G. Raleigh, J. M. Cioffi, "Spatio-temporal coding for wireless communications," in Proceedings of the *1996 Global Telecommunications Conference* (*GLOBECOM)*, vol. 3, pp. 1809-1814, Nov. 1996.

[4] G. J. Foschini, "Layered space-time architecture for wireless communication in a fading environment when using multi-element antennas," in *Bell Labs Technical Journal*, vol. 1, no. 2, pp. 41-59, Sep. 1996.

[5] A. J. Goldsmith, Wireless Communications, 1st ed., New York: Cambridge University Press, 2005.

[6] M. Chiani, M. Z. Win, and A. Zanella, "On the Capacity of Spatially Correlated MIMO Rayleigh-Fading Channels," in *IEEE Transactions on Information Theory*, vol. 49, no. 10, pp. 2363-2371, Oct. 2003.

[7] D. Shiu, G. J. Foschini, M. J. Gans, J. M. Kahn, "Fading correlation and its effect on the capacity of multielement antenna systems," in *IEEE Transactions on Communications*, vol. 48, no. 3, pp. 502-513, Mar. 2000.

[8] P. W. Wolniansky, G. J. Foschini, G. D. Golden, and R. A. Valenzuela, "V-BLAST: An Architecture for Realizing very High Data Rates over the Rich-Scattering Wireless Channel," in Proceedings of the *URSI International Symposium on Signals, Systems and Electronics (ISSSE)*, pp. 295-300, Sep./Oct. 1998.

[9] R. Y. Mesleh, H. Haas, S. Sinanovic, C. W. Ahn, S. Yun, "Spatial Modulation," in *IEEE Transactions on in Vehicular Technology*, vol. 57, no. 4, pp. 2228-2241, Jul. 2008.

[10] A. Goldsmith, S. A. Jafar, N. Jindal, S. Vishwanath, "Capacity Limits of MIMO Channels," in *IEEE Selected Areas in Communications*, vol. 21, no. 5, pp. 684-702, Jun. 2003.

[11] M. O. Damen, A. Abdi, K. Mostafa, "On the effect of correlated fading on several space-time coding and detection schemes," in Proceedings of the 54th *IEEE Vehicular Technology Conference (VTC)*, vol. 1, pp. 13-16, Sep./Oct. 2001.

[12] R. Y. Mesleh, H. Haas, C. W. Ahn, S. Yun, "Spatial Modulation - A New Low Complexity Spectral Efficiency Enhancing Technique," in Proceedings of the *2006 First International Conference on Communications and Networking in China (ChinaCom)*, pp. 1-5, Oct. 2006.

[13] J. Jeganathan, A. Ghrayeb, L. Szczecinski, "Spatial modulation: optimal detection and performance analysis," in *IEEE Communications Letters*, vol. 12, no. 8, pp. 545-547, Aug. 2008.

[14] N. R. Naidoo, H. Xu, T. Quazi, "Spatial modulation: optimal detector asymptotic performance and multiple-stage detection," in *IET Communications*, vol. 5, no. 10, pp. 1368-1376, Jul. 2011.

[15] Q. Tang, Y. Xiao, P. Yang, Q. Yu, S. Li, "A New Low-Complexity Near-ML Detection Algorithm for Spatial Modulation," in *IEEE Transactions on Wireless Communications Letters*, vol. 2, no. 1, pp. 90-93, Feb. 2013.

[16] S. Hwang, S. Jeon, S. Lee, and J. Seo, "Soft-ouput ML detector for spatial modulation OFDM systems," *IEICE Electronics Express*, vol. 6, no. 19, pp. 1426-1431, Oct. 2009.

[17] A. Younis, R. Mesleh, H. Haas, P. M. Grant, "Reduced Complexity Sphere Decoder for Spatial Modulation Detection Receivers," in Proceedings of the *2010 IEEE Global Telecommunications Conference (GLOBECOM)*, pp. 1-5, 6-10 Dec. 2010.

[18] J. Wang, S. Jia, J. Song, "Signal Vector Based Detection Scheme for Spatial Modulation," in *IEEE Communications Letters*, vol. 16, no. 1, pp. 19-21, Jan. 2012.

[19] N. Pillay, H. Xu, "Comments on "Signal Vector Based Detection Scheme for Spatial Modulation"," in *IEEE Communications Letters*, vol. 17, no. 1, pp. 2-3, Jan. 2013.

[20] J. Zheng, "Signal Vector Based List Detection for Spatial Modulation," in *IEEE Transactions on Wireless Communications Letters*, vol. 1, no. 4, pp. 265-267, Aug. 2012.

[21] J. Jeganathan, A. Ghrayeb, and L. Szczecinski, "Space Shift Keying Modulation for MIMO Channels," in *IEEE Transactions on Wireless Communications*, vol. 8, no. 7, pp. 3692-3703, Jul. 2009.

[22] H. Liang, R. Y. Chang, W. Chung, H. Zhang, S. Kuo, "Bi-Space Shift Keying Modulation for MIMO Systems," in *IEEE Communications Letters*, vol. 16, no. 8, pp. 1161-1164, Aug. 2012.

[23] S. Ganesan, R. Mesleh, H. Haas, C. W. Ahn, S. Yun, "On the Performance of Spatial Modulation OFDM," in Proceedings of the *2006 Asilomar Conference on Signals, Systems and Computers (ACSSC)*, pp. 1825-1829, Nov. 2006.

[24] R. Mesleh, S. Ganesan, H. Haas, "Impact of Channel Imperfections on Spatial Modulation OFDM," in Proceedings of the *IEEE 18th International Symposium on Personal, Indoor and Mobile Radio Communications (PIMRC)*, pp. 1-5, Sep. 2007.

[25] N. Serafimovski, M. D. Renzo, S. Sinanovic, R. Y. Mesleh, and H. Haas, "Fractional Bit Encoded Spatial Modulation (FBE-SM)," in *IEEE Communications Letters*, vol. 14, no. 5, pp. 429-431, May 2010.

[26] A. Younis, N. Serafimovski, R. Y. Mesleh, H. Haas, "Generalised spatial modulation," in Proceedings of the *2010 Conference Record of the Forty Fourth Asilomar Conference on Signals, Systems and Computers (ASILOMAR*), pp. 1498-1502, Nov. 2010.

[27] J. Jeganathan, A. Ghrayeb, L. Szczecinski, "Generalized space shift keying modulation for MIMO channels, " in Proceedings of the *IEEE 19th International Symposium on Personal, Indoor and Mobile Radio Communications (PIMRC) 2008*, pp. 1-5, Sep. 2008.

[28] J. Wang, S. Jia, J. Song, "Generalised Spatial Modulation System with Multiple Active Transmit Antennas and Low Complexity Detection Scheme," in *IEEE Transactions on Wireless Communications*, vol. 11, no. 4, pp. 1605-1615, Apr. 2012.

[29] E. Basar, U. Aygolu, E. Panayirci, and H. V. Poor, "Space-Time Block Coded Spatial Modulation," in *IEEE Transactions on Communications*, vol. 59, no. 3, pp. 823-832, Mar. 2011.

[30] R. Y. Mesleh, S. S. Ikki, H. M. Aggoune, "Quadrature Spatial Modulation," in *IEEE Transactions on Vehicular Technology*, vol. 64, no. 6, pp. 2738-2742, Jun. 2015.

[31] R. Y. Mesleh, S. S. Ikki, "On the impact of imperfect channel knowledge on the performance of quadrature spatial modulation," in Proceedings of the *2015 IEEE Wireless Communications and Networking Conference (WCNC)*, pp. 534-538, Mar. 2015.

[32] P. Yang, Y. Xiao, Y. Yu, and S. Li, "Adaptive Spatial Modulation for Wireless MIMO Transmission Systems," in *IEEE Communications Letters*, vol. 15, no. 6, pp. 602-604, Jun. 2011.

[33] P. Yang, Y. Xiao, L. Li, Q. Tang, Y. Yu, and S. Li, "Link Adaptation for Spatial Modulation with Limited Feedback," in *IEEE Transactions on Vehicular Technology*, vol. 61, no. 8, pp. 3808-3813, Oct. 2012.

[34] R. W. Health, S. Sandhu, A. Paulraj, "Antenna Selection for Spatial Multiplexing Systems with Linear Receivers," in *IEEE Communications Letters*, vol. 5, no. 4, pp. 142-144, Apr. 2001.

[35] R. W. Health, A. Paulraj, "Antenna Selection for Spatial Multiplexing Systems based on Minimum Error Rate," in Proceedings of the 2001 *IEEE International Conference on Communications (ICC)*, vol. 7, pp. 2276-2280, Jun. 2001.

[36] S. Sanayei, A. Nosratinia, "Antenna selection in MIMO systems," in *IEEE Communications Magazine*, vol. 42, no. 10, pp. 68-73, Oct. 2004.

[37] D. A. Gore, R. U. Nabar, A. Paulraj, "Selecting an optimal set of transmit antennas for a low rank matrix channel," in Proceedings of the 2000 *IEEE International Conference on Acoustics, Speech, and Signal Processing (ICASSP)*, vol. 5, pp. 2785-2788, Jun. 2000.

[38] J. Jeganathan, "Space shift keying modulation for MIMO channels," M.S. thesis, Dept. Elect. Eng., Concordia Univ., Montreal, QC, Canada, Aug. 2008.

[39] R. Rajashekar, K. V. S. Hari, and L. Hanzo, "Antenna Selection in Spatial Modulation Systems," in *IEEE Communications Letters*, vol. 17, no. 3, pp. 521-524, Mar. 2013.

[40] R. Rajashekar, K. V. S. Hari and L. Hanzo, "Quantifying the Transmit Diversity Order of Euclidean Distance Based Antenna Selection in Spatial Modulation," in *IEEE Signal Processing Letters*, vol. 22, no. 9, pp. 1434-1437, Sep. 2015.

[41] N. Pillay and H. Xu, "Comments on "Antenna Selection in Spatial Modulation Systems"," in *IEEE Communications Letters*, vol. 17, no. 9, pp. 1681-1683, Sep. 2013.

[42] N. Pillay, H. Xu, "Low-complexity transmit antenna selection schemes for spatial modulation," in *IET Communications*, vol. 9, no. 2, pp. 239-248, Jan. 2015.

[43] S. Naidu, N. Pillay, H. Xu, "A Study of Quadrature Spatial Modulation," in Proceedings of the *Southern Africa Telecommunications Network and Applications Conference (SATNAC)*, pp. 3-8, Aug. 2015.

[44] Z. Zhou, N. Ge, X. Lin, "Reduced-Complexity Antenna Selection Schemes in Spatial Modulation," in *IEEE Communications Letters*, vol. 18, no. 1, pp. 14-17, Jan. 2014.

[45] K. Ntontin, M. Di Renzo, A. I. Perez-Neira, C. Verikoukis, "A Low-Complexity Method for Antenna Selection in Spatial Modulation Systems," in *IEEE Communications Letters*, vol. 17, no. 12, pp. 2312-2315, Dec. 2013.